In silico identification of metabolic enzyme drug targets in *Burkholderia pseudomallei*

Jean F. Challacombe [1]*

[1] Bioscience Division, Los Alamos National Laboratory, Los Alamos, NM 87545; jchalla@lanl.gov
* Correspondence: jchalla@lanl.gov; Tel.: +1-505-665-1485

Abstract: The intracellular pathogen *Burkholderia pseudomallei,* which is endemic to parts of southeast Asia and northern Australia, causes the disease melioidosis. Although acute infections can be treated with antibiotics, melioidosis is difficult to cure, and some patients develop chronic infections or a recrudescence of the disease months or years after treatment of the initial infection. *B. pseudomallei* strains have a high level of natural resistance to a variety of antibiotics, and with limited options for new antibiotics on the horizon, new alternatives are needed. The aim of the present study was to characterize the metabolic capabilities of *B. pseudomallei*, identify metabolites crucial for pathogen survival, understand the metabolic interactions that occur between pathogen and host cells, and determine if metabolic enzymes produced by the pathogen might be potential antibacterial targets. This aim was accomplished through genome scale metabolic modeling under different external conditions: 1) including all nutrients that could be consumed by the model, and 2) providing only the nutrients available in culture media. Using this approach, candidate chokepoint enzymes were identified, then knocked out *in silico* under the different nutrient conditions. The effect of each knockout on the metabolic network was examined. When five of the candidate chokepoints were knocked out *in silico*, the flux through the *B. pseudomallei* network was decreased, depending on the nutrient conditions. These results demonstrate the utility of genome-scale metabolic modeling methods for drug target identification in *B. pseudomallei*.

Keywords: Burkholderia, pathogen, metabolism, metabolic network, nutrients, infection

1. Introduction

The intracellular pathogen *Burkholderia pseudomallei,* which causes the disease melioidosis, is acquired from the environment in parts of southeast Asia and northern Australia [1,2]. Although acute infections can be treated with antibiotics, melioidosis is difficult to cure, requiring lengthy treatment in two phases for a duration of ~20 weeks [3,4]. Despite antibiotic therapy, some patients have persistent cases that develop into chronic infections, and others experience a recrudescence of the disease months or years after treatment of the initial infection with antibiotics [5]. *B. pseudomallei* strains have a high level of natural resistance to a variety of antibiotics [6-8], and with limited options for new antibiotics on the horizon, alternatives are desperately needed.

The availability of many *B. pseudomallei* genomes and advances in computational analysis methods make possible the rapid identification of novel antibacterial targets by selecting the most likely targets from complete sets of protein coding genes. Previous studies have demonstrated that essential genes present in pathogen genomes, but not in the host, make the best therapeutic targets [9]. Many known antibacterial compounds are enzyme inhibitors [10,11], so metabolic enzymes specific to pathogenic bacteria represent promising drug targets [9].

Enzyme targets in key metabolic pathways have been identified in *B. pseudomallei* and other bacterial pathogens; these pathways include fatty acid biosynthesis [12-14], the glyoxalate shunt [15,16], the chorismate pathway for biosynthesis of aromatic amino acids [17], purine, histidine, 4-aminobenzoate, and lipoate biosynthesis [18,19], leucine, threonine, p-aminobenzoic acid, aromatic

compound biosynthesis [20], branched chain amino acid biosynthesis [21], purine metabolism [22]. Other enzyme targets have been identified that are not in pathways - alanine racemase (interconverts L- and D-alanine) [23], superoxide dismutase [24] and cyclic di-GMP phosphodiesterase [25].

Drugs acting on pathogen targets that are not present in the host should not cause significant side effects. However, before the human genome was available, the process of identifying bacterial pathogen-specific drug targets was labor intensive, involving comparison of candidate pathogen targets against all known eukaryotic sequences to filter out targets likely to occur in the human [9]. Since then, various software tools have made the process of *in silico* target identification in pathogen genomes easier. Available *in silico* tools encompass various cheminformatic [26] and bioinformatic [27,28] approaches to identify new protein targets. Among the bioinformatic tools, metabolic pathway/metabolic network analysis has emerged as an efficient *in silico* method to identify candidate metabolic enzyme targets in pathogen genomes.

Several software packages are available to facilitate genome-scale metabolic network analyses [29]. Starting with an annotated pathogen genome, the components of metabolic pathways are identified, curated and refined [30]. The resulting genome-scale metabolic model can be used to integrate omics datasets and to perform various analyses to determine the most likely drug targets [10]. Perhaps the most important task with respect to finding good candidate targets is metabolic chokepoint identification. By definition, a chokepoint enzyme either consumes a unique substrate or produces a unique product in the pathogen metabolic network [31]. Inhibition of chokepoint enzymes may disrupt crucial metabolic processes in the pathogen, so chokepoints that are essential to the pathogen represent good potential drug targets [32-34].

The aim of the present study was to characterize the metabolic capabilities of *B. pseudomallei*, identify metabolites and aspects of the metabolic network crucial for pathogen survival, understand the metabolic interactions that occur between pathogen and host cells, and determine if any of the metabolic enzymes produced by the pathogen might be potential antibacterial targets. This aim was accomplished through genome scale metabolic modeling of *B. pseudomallei* under different external conditions, including all nutrients that could be consumed by the model and only the nutrients available in culture media. Using this approach, candidate chokepoints were identified, then knocked out the genes encoding chokepoint enzymes *in silico* under the different nutrient conditions, and examined the effect of each knockout on the metabolic network. The result of this analysis was five candidate antibacterial targets, demonstrating the utility of genome-scale metabolic modeling methods for *in silico* studies of pathogen metabolism and for drug target identification in *B. pseudomallei*.

2. Materials and Methods

2.1 Metabolic pathway reconstructions and annotation curation

Pathway genome databases (PGDBs) for *B. pseudomallei* strains MSHR668 and K96243 were obtained through the Pathway Tools software (version 18.5) from the PGDB registry [35]. We found that the original annotation of *B. pseudomallei* K96243 identified many fewer coding sequences than that of MSHR668, so we re-annotated the original complete genome sequences of both strains using the RAST system [36] to better compare them [37]. The RAST-annotated genome sequences were loaded into Pathway Tools, using the PathoLogic component to predict the metabolic pathways [38]. For each genome, the set of protein coding sequences from the original annotation was compared to those from the RAST annotation, using blast to identify coding sequences in common between the two annotations, and to identify coding sequences that were missing from each annotation. For the MSHR668 genome, RAST annotation identified 247 fewer coding sequences than the original annotation. However, there were some predicted coding sequences with annotated functions in the RAST annotation that were not present in the original, so these were added to the original PGDB for MSHR668. The RAST annotation of the K96243 genome identified 1,317 more protein coding sequences than the original annotation, so the PGDB created from the RAST annotation was used as the starting point. Coding sequences from the original annotation that were not present in the RAST annotation of K96243 were added to the PGDB that was created from the RAST annotated genome.

97
98 *2.2 Chokepoint Identification*
99 Chokepoints were identified in each PGDB using the chokepoint reaction finder in Pathway
100 Tools. All reactions were included except those found in human.
101
102 *2.3 Flux balance analysis*
103 For each metabolic network reconstruction, flux balance analysis (FBA) was performed using
104 the MetaFlux module within the Pathway Tools [39]. Development FBA models were constructed
105 iteratively to determine the compounds that each model could use and produce. This was
106 accomplished by trying all compounds in the PGDB as biomass metabolites, nutrients and secretions
107 in the various compartments (cytosol, periplasmic space and extracellular). Each model was refined
108 iteratively, first identifying the specific biomass components that could be produced, then trying all
109 compounds as nutrients and secretions, then specifying the biomass metabolites and nutrients and
110 trying all compounds as secretions.
111 Once the nutrients, secretions and biomass components that could be consumed or produced by
112 the metabolic networks were determined, the log file produced by MetaFlux was examined and
113 problematic reactions were fixed, if possible. Most of the problematic reactions were unbalanced due
114 to missing chemical formulas of one or more metabolites. A few of these reactions were corrected by
115 copying the missing structures from other PGDBs. For example, the structures of D-ribose, D-
116 glucuronate, D-glucose and some other compounds were copied from the more highly curated
117 *Escherichia coli* K12 substr. MG1655 PGDB. Many of the reactions with compounds that were lacking
118 chemical formulas were generic so no suitable chemical structure could be found or created.
119 Reactions involving starch, glycogen, and glucans with variable lengths and non-numeric
120 stoichiometries, could not be balanced. Other reactions were missing H^+ or H_2O on one side or the
121 other, and the addition of the missing compound balanced the reaction. However, there were a small
122 number of reactions that could not be fixed and these were marked as unbalanced. Once all reactions
123 that could be fixed were corrected in the PGDB, MetaFlux was run again in development mode to
124 identify additional biomass metabolites, nutrients, and secretions. Once the set of biomass
125 metabolites was constant, the nutrients that could be consumed by the model were determined,
126 followed by identification of the secretions produced by the model. The result of this process was a
127 final unconstrained FBA model.
128 To mimic the nutrient conditions in culture, only the estimated set of ingredients present in LB
129 medium were included as nutrients in the FBA model. LB medium includes as its main ingredients
130 tryptone [40] and yeast extract [41]. Tryptone provides peptides and peptones, which are good
131 sources of amino acids (http://www.sigmaaldrich.com/analytical-
132 chromatography/microbiology/basic-ingredients/protein-sources.html); yeast extract provides
133 vitamins, nitrogenous compounds, carbon, sulfur, trace elements and minerals [42]. The LB media
134 composition reported in a *Bacillus subtilis* modeling study [43] was used as a starting point for this
135 study. Starting with the nutrient set that mimicked LB media [43], all compounds were included in
136 the try-biomass set for the cytosol and periplasmic cellular compartments to see which biomass
137 metabolites could be produced given only the nutrients present in LB media. Once a stable set of
138 nutrients was determined, iterations were performed to determine the stable set of biomass
139 metabolites that could be produced. Then all compounds were tried as secretions in the cytosol and
140 periplasmic compartments to determine the compounds that could be secreted by the model.
141 A list of nutrients that might be available to *B. pseudomallei* while residing inside host cells during
142 infection was compiled by searching the literature for infection studies involving *B. pseudomallei* and
143 host cells. Gene expression studies of other intracellular pathogens and host cells during infection
144 were also considered. A development FBA model mimicking infection conditions was constructed as
145 described above for the LB media model.
146
147 *2.4 Essential gene and candidate drug target identification*

To reduce the set of potential drug targets, candidate chokepoint enzymes were compared against the list of essential genes and all of the drug targets in DrugBank. Essential genes in the MSHR668 genome were determined by blasting all protein coding sequences (amino acid format) against the Database of Essential Genes [44] using the blastp program with an E-value cut-off of 1e -10 and 70% identity as thresholds. Candidate drug target sequences were determined by blasting all protein coding sequences in the MSHR668 genome (as both nucleotide and amino acid formats) against the complete set of DrugBank targets [45], using an E-value cutoff of 0.005 and a threshold identity of 70% to select likely targets.

2.5 In silico knockout experiments

Knockout experiments were performed *in silico* through the Pathway Tools MetaFlux module [39]; the chokepoint genes were knocked out one at a time and the effects on total biomass flux through the metabolic network were noted.

2.6 Network visualization

For each PGDB, an .sbml file was exported from the Pathway Tools and loaded into Cytoscape [46] version 3.1.1 for visualization and comparison of network features.

3. Results

3.1. General features of B. pseudomallei genomes and metabolic networks

The general characteristics of each PGDB and metabolic network for B. pseudomallei MSHR668 and K96243 are listed in Table 1.

Table 1. Features of *B. pseudomallei* PGDBs and metabolic networks

Genome (Pathway Tools PGDB)	**Curated MSHR668 (original + RAST)**	**Curated K96243 (RAST + original)**
Coding sequences	7133	7045
Pathways	339	387
Enzymatic reactions	1870	1995
Transport reactions	144	82
Enzymes	1666	1685
Transporters	292	38
Compounds	1397	1578
Metabolic Network		
Nodes (metabolites)	4295	4219
Edges (reaction steps)	10860	9747
Chokepoints		
Producing	444	506
Consuming	419	498
Candidate	479	348
Dead-end reactants	166	217
Dead-end products	72	118

The *B. pseudomallei* MSHR668 and K96243 genomes contained similar numbers of coding sequences, pathways, enzymatic reactions and enzymes. Differences between the PGDBs were noted in the numbers of transporters, transport reactions and compounds. The K96243 PGDB contained fewer transporters and transport reactions and more compounds than MSHR668. In terms of the metabolic network characteristics, both networks contained similar numbers of nodes (representing metabolites), while the MSHR668 network had more edges (reaction steps) than K96243. This is likely

due to the more extensive curation of the MSHR668 network that was performed during refinement of the metabolic network models (see Methods).

In a metabolic network, chokepoints are reactions that either uniquely produce or uniquely consume a metabolite. Inhibiting an enzyme that consumes a unique substrate may cause that metabolite to accumulate, and it may be toxic to the cell; inhibiting an enzyme that produces a unique product may starve the cell of an essential metabolite [31]. Identifying chokepoint enzymes in pathogens is a promising *in silico* approach to recognize potential metabolic drug targets. For example, analysis of *Plasmodium falciparum* metabolism revealed that 87.5% of proposed drug targets supported by evidence are chokepoint reactions [31]. However, to be a valid chokepoint, the metabolite in question must be balanced by a producing or consuming reaction and not be a dead-end metabolite [31]. Table 1 compares the numbers of chokepoint reactions and dead-end metabolites that were identified in each PGDB. Overall the numbers were similar between the two PGDBs, and the lower numbers of dead-ends in the MSHR668 database were likely due to the more extensive curation performed on the MSHR668 PGDB (see Materials and Methods).

3.2. Flux balance analysis (FBA)

3.2.1. Unconstrained FBA model

Given a set of nutrients for consumption, along with secretions and metabolites that can be produced, a FBA model predicts the steady-state flux rates of the metabolic reactions in an organism, and provides an estimate of the overall biomass flux. FBA was conducted on each metabolic network as described in the Materials and Methods section. It took several cycles of refinement to solve an initial unconstrained MSHR668 model. Even after several iterations, the K96243 unconstrained model did not reach a stable solution, likely because there were missing transporter-encoding genes (and possibly other genes) in the PGDB, indicating that the annotation needed more curation. Since the unconstrained MSHR668 model reached a stable solution after performing the initial network curation steps suggested by MetaFlux, only this model was analyzed further. The initial unconstrained FBA model of the MSHR668 metabolic network (Table 2) included all possible biomass compounds that could be produced, all nutrients that could be consumed, and had no weights imposed on the biomass metabolites and no constraints imposed on the nutrients. [Supplementary materials, S1_Final_unconstrained_model_inputs.pdf, S2_Final_unconstrained_model_solution.pdf].

3.2.2. LB media FBA model

To mimic the conditions that *B. pseudomallei* experiences in culture, only the nutrients present in LB media [43] plus glycerol were included as inputs to the LB media FBA model (Table 2). In this model, constraints were included on some of the nutrients (ADP, Pi, proton and glycerol). [Supplementary materials, S3_Final_LB_model_inputs.pdf and S4_Final_LB_model_solution.pdf].

Table 2. Characteristics of the MSHR668 unconstrained and LB media models

Model	Total rxns	Rxns carrying flux	Biomass metabolites produced	Nutrients consumed	Secre-tions	Biomass flux
Unconstrained	3193	1619	1403	667	10	15000.00
LB media	3213	1025	282	47	0	0.079412

3.2.3. Host cell infection model

In addition to the unconstrained and LB media models, the original plan for this study included the development of a model of *B. pseudomallei* metabolism that mimics infection conditions. However, there was very little information available on the growth requirements of *B. pseudomallei* inside human macrophages. In addition, no comprehensive studies have been performed to identify the complete list of host cell nutrients that are available to *B. pseudomallei* during infection. Most studies of the nutritional requirements of intracellular pathogens growing inside host cells have been performed on *Legionella pneumophila* [47,48], which can grow and replicate similarly in human macrophages and amoebae [49]. Growing in both human macrophages and amoebae, *L. pneumophila* utilizes amino acids as its main sources of carbon, nitrogen and energy; *L. pneumophila* obtains amino acids from the host through proteasomal degradation [48]. However, glucose is also used to feed central metabolism under both culture and infection conditions [50].

Comparing the nutrients provided by the LB media model to the nutrients used by *L. pneumophila* in culture and during infection of amoebae [47], the only difference was the carbohydrate carbon source: glycerol (*B. pseudomallei* LB media [51]) vs. glucose (*L. pneumophila* AYE media [50] and in amoebae [47,50]). When glycerol was replaced by glucose in the LB media model of *B. pseudomallei*, no FBA solution was found [data not shown]. Several possible explanations for this result are presented in the Discussion.

While the specific carbon requirements of *B. pseudomallei* in either human macrophages or amoebae have not been determined, one study produced whole-genome tiling array expression data to assess *B. pseudomallei* transcriptional responses under 82 different conditions, including infection [52]. From their supplemental table S2, a list of metabolic genes expressed in the infection conditions was used to infer the potential nutrients consumed by *B. pseudomallei* during infection. Additional candidate host cell nutrients were identified from the literature, focusing on studies of intracellular pathogen-mammalian host infections. The nutrients identified as potential carbon sources for intracellular survival of various pathogens included aromatic compounds, such as benzoate and phenylacetic acid and related derivatives [53], sugar acids like gluconate, galactonate, glucuronate, and galacturonate [54], ribo- and deoxyribonucleosides, hexuronates [55], glutathione [56], glucose 6-phosphate [57,58], glycerol-3-phosphate [59]. The complete list of potential host cell nutrients is in the [Supplementary material, S5_Nutrients_infection_model.pdf] file.

FBA was performed for a *B. pseudomallei* MSHR668 model that included the list of candidate host cell nutrients identified as above. However, some of the nutrients were not present in any reactions in the MSHR668 PGDB. When the rest of the compounds were included as nutrients in addition to glycerol, none of them were consumed by the model, but glycerol was consumed and biomass was produced. When glycerol was excluded from the nutrient list, none of the other nutrients were consumed and the model was not solvable [data not shown].

3.3. Metabolic chokepoints and candidate drug targets

To narrow down the list of metabolic chokepoints, which represented candidate drug targets, essential genes and genes with sequence homology to existing DrugBank targets were identified in the MSHR668 genome. This analysis identified 34 chokepoint genes that were also essential genes and DrugBank targets (Figure 1, Table 3).

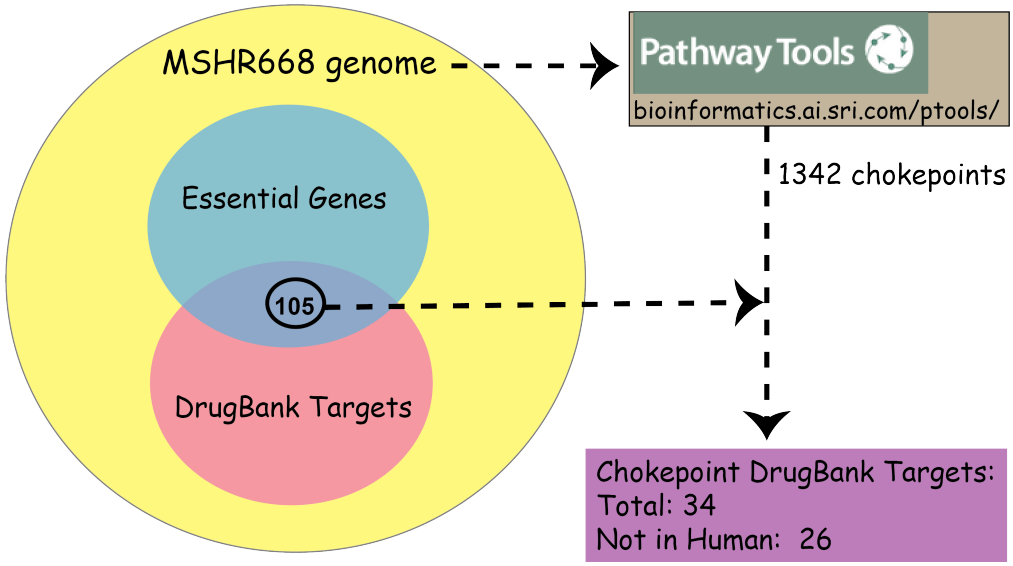

Figure 1. Process for identifying candidate metabolic enzyme drug targets (chokepoints) in the *B. pseudomallei* MSHR668 genome.

Table 3. Chokepoint genes that encode candidate metabolic enzyme drug targets in *B. pseudomallei* MSHR668

Locus_tag	Gene symbol	Enzyme name	E.C. number	DrugBank target (drug IDs)	Human target?	Choke-point in K96243?	Bp Mutant(s) exist?
BURPS668_0305	argG⁺	argininosuccinate synthase	6.3.4.5	P0A6E4 Argininosuccinate synthase (DB00536; DB04077)	no	yes	no*
BURPS668_0328	folB⁺	dihydroneopterin aldolase	4.1.2.25	P56740 Dihydroneopterin aldolase (DB01778; DB01906; DB02119; DB02489; DB03231; DB03571; DB04168; DB04400; DB04425; DB06906)	no	yes	no
BURPS668_0567	pth⁺	peptidyl-tRNA hydrolase	3.1.1.29	No	yes	yes	no
BURPS668_0675	aspS⁺	aspartyl-tRNA synthase	6.1.1.12	P36419 Aspartate—tRNA ligase (DB01895)	no	no	no

BURPS668_0810	RecA+	RecA protein	5.99.1.-	P62219 RecA (DB01660; DB03222; DB04444; DB04395)	no	yes	no*
BURPS668_0964	dut+	deoxyuridine5'-triphosphate nucleotidohydrolase	3.6.1.19/ 3.6.1.23	P06968 Deoxyuridine 5'-triphosphate nucleotidohydrolase (DB01965; DB02333; DB03413; DB03800)	no	yes	no
BURPS668_0967	ileS+	isoleucyl-tRNA synthetase	6.1.1.5	Q9NSE4 Isoleucine--tRNA ligase (DB00167)	yes	no	no
BURPS668_1446	pckG+	phosphoenolpyruvate carboxykinase	4.1.1.32	P35558 Phosphoenolpyruvate carboxykinase, cytosolic [GTP] (DB01819; DB02008; DB03267; DB03725)	yes	yes	no
BURPS668_1465	dnaQ+	DNA polymerase III subunit epsilon	2.7.7.7	P03007 DNA polymerase III subunit epsilon (DB01643)	no	yes	no
BURPS668_1544	NA+	alpha-glucosidase	3.2.1.20	O33830 Alpha-glucosidase (DG01769; DB03323)	yes lysosomal	no	no
BURPS668_1669	valS+	valyl-tRNA synthetase	6.1.1.9	P26640 Valine--tRNA ligase (DB00161)	yes	no	no
BURPS668_1712	thrS+	threonyl-tRNA synthetase	6.1.1.3	P0A8M5 Threonine--tRNA ligase (DB03355; DB03869; DB04024)	no	no	no
BURPS668_1750	sucA+	2-oxoglutarate dehydrogenase E1	1.2.4.2	Q02218 2-oxoglutarate dehydrogenase, mitochondrial (DB00157; DB00313)	yes	yes	no
BURPS668_1752	lpdA+	dihydrolipoamide	1.8.1.4	P14218 Dihydrolipoyl	no	yes	no

		dehydrogenase		dehydrogenase (DB03147)			
BURPS668_2178	purA+	adenylosuccinate synthetase	6.3.4.4	Q83P33 Adenylosuccinate synthetase (DB02954; DB04160; DB04566)	no	yes	no
BURPS668_2189	hisS+	histidyl-tRNA synthetase	6.1.1.21	P60906 Histidine--tRNA ligase (DB03811; DB04201)	no	no	no
BURPS668_2308	pgi+	glucose-6-phosphate isomerase	5.3.1.9	P06744 Glucose-6-phosphate isomerase (DB02007; DB02076; DB02093; DB02548; DB03042; DB03581; DB03937; DB04493)	yes	no	no
BURPS668_2426	lpxD+	UDP-3-O-[3-hydroxymyristoyl] glucosamine N-acyltransferase	2.3.1.191	O67648 UDP-3-O-[3-hydroxymyristoyl] N-acetylglucosamine deacetylase (DB01991; DB04257; DB04399; DB07355; DB07536; DB08231; DB07861)	no	yes	no
BURPS668_2433	uppS+	undecaprenyl diphosphate synthase	2.5.1.31	P60472 Ditrans,polycis-undecaprenyl-diphosphate synthase ((2E,6E)-farnesyl-diphosphate specific) (DB04695; DB04714; DB07404; DB07409; DB07410; DB07426; DB07780)	no	yes	no

BURPS668_2610	lpdA+	pyruvate dehydrogenase complex E3 component, dihydrolipoamide dehydrogenase	1.8.1.4	P10802 Dihydrolipoyllysine-residue acetyltransferase component of pyruvate dehydrogenase complex (DB01846; DB01992; DB08120)	no	yes	no
BURPS668_2788	fabF+	3-oxoacyl-ACP synthase	2.3.1.41	Q02054 Actinorhodin polyketide synthase acyl carrier protein (DB08585; DB08586)	no	no	no
BURPS668_3103	rfbA+	glucose-1-phosphate thymidylyltransferase	2.7.7.24	Q9HU22 Glucose-1-phosphate thymidylyltransferase (DB01643; DB02452; DB02843; DB03723; DB03751; DB04272; DB04485; DB02452; DB04355)	no	yes	no
BURPS668_3328	tgt+	queuine tRNA-ribosyltransferase	2.4.2.29	P28720 Queuine tRNA-ribosyltransferase (DB01825; DB02041; DB02441; DB02599; DB03074; DB03304; DB03505; DB03780; DB04004; DB04169; DB04239; DB04543; DB07012; DB07452; DB07481; DB07564; DB07704; DB08267;	no	yes	no

				DB08268; DB08511; DB08512; DB08514)			
BURPS668_3366	ruvB+	Holliday junction DNA helicase RuvB	3.1.22.4	Q5SL87 Holliday junction ATP-dependent DNA helicase RuvB (DB00173)	no	no	no
BURPS668_3464	aroQ+	3-dehydroquinate dehydratase	4.2.1.10	P15474 3-dehydroquinate dehydratase (DB02786; DB02801; DB04347; DB04656; DB08485)	no	yes	no
BURPS668_3525	murG+	undecaprenyldiphospho-muramoylpentapeptide beta-N-acetylglucosaminyltransferase	2.4.1.227	P17443 UDP-N-acetylglucosamine--N-acetylmuramyl-(pentapeptide)pyrophosphoryl-undecaprenol N-acetylglucosamine transferase (DB02196)	no	yes	no
BURPS668_3561	ung+	uracil-DNA glycosylase	3.2.2.27	Q8X444 Uracil-DNA glycosylase (DB03419)	no	yes	no
BURPS668_3668	murA+	UDP-N-acetylglucosamine 1-carboxyvinyltransferase		P33038 UDP-N-acetylglucosamine 1-carboxyvinyltransferase (DB01879; DB02435; DB02995; DB03089; DB04174; DB04474)	no	yes	no
BURPS668_A0384	acnD+	aconitate hydratase	4.2.1.3	Q99798 Aconitate hydratase, mitochondrial (DB01727; DB03964; DB04072; DB04351;	yes	yes	no

				DB04562); P36683 Aconitate hydratase 2 (DB04351)			
BURPS668_A1869	ileS+	isoleucyl-tRNA synthetase	6.1.1.5	P41972 isoleucyl-tRNA synthetase (DB00410)	no	no	no
BURPS668_A2053	NA+	putative acetyl-CoA carboxylase, biotin carboxylase	6.3.4.14	P24182 Biotin carboxylase (DB08074; DB08075; DB08076; DB08144; DB08145; DB08146; DB08314; DB08315; DB08316; DB08317; DB08318)	no	yes	no
BURPS668_A2451	leuB+	3-isopropylmalate dehydrogenase	1.1.1.85	Q56268 3-isopropylmalate dehydrogenase (DB04279)	no	yes	no
BURPS668_A2546	polA+	DNA polymerase I	2.7.7.7	P00582 DNA polymerase I (DB00548; DB08432)	no	yes	no
BURPS668_A3190	lpdA+	dihydrolipoamide dehydrogenase	1.8.1.4	P09063 Dihydrolipoyl dehydrogenase (DB03147)	no	yes	no

* mutants exist in other *Burkholderia* species, +essential gene in *B. pseudomallei* K96243 and MSHR668

Eight of the targets in Table 3 were also DrugBank targets in human; DrugBank was searched for the remaining twenty-six targets, showing that they also occur in other bacteria.

In silico knockout experiments were performed with the MetaFlux module of Pathway Tools to test the effect of inhibiting each chokepoint enzyme on *B. pseudomallei* growth in both the unconstrained and LB media models. Results (Table 4) show that knockout of BURPS668_3328 (*tgt*) and BURPS668_A2451 (*leuB*), eliminated the biomass flux in the unconstrained model, while knockout of BURPS668_2426 (*lpxD*), BURPS668_2433 (*uppS*), and BURPS668_3525 (*murG*) eliminated the biomass flux in the LB media model. Knockout of BURPS668_2433 (*uppS*), and BURPS668_3525 (*murG*) decreased the biomass flux in the unconstrained model, but did not eliminate it.

Table 4. Results of *in silico* knockout experiments on twenty-six chokepoint reactions in *B. pseudomallei*

locus_tag	Gene name	Reaction(s)	Biomass flux (unconstrained model)	Biomass flux (LB media model)
BURPS668_0305	argG	ARGSUCCINSYN-RXN	15000.000000	0.079412
BURPS668_0328	folB	H2NEOPTERINALDOL-RXN	15000.000000	0.079412
BURPS668_0675	aspS	ASPARTATE--TRNA-LIGASE-RXN-ASP-tRNAs/L-ASPARTATE/ATP/PROTON//Charged-ASP-tRNAs/AMP/PPI.60	15000.000000	0.079412
BURPS668_0810	recA	RXN0-5100	15000.000000	0.079412
BURPS668_0964	dut	DUTP-PYROP-RXN	15000.000000	0.079412
BURPS668_1465	dnaQ	DNA-DIRECTED-DNA-POLYMERASE-RXN	15000.000000	0.079412
BURPS668_1712	thrS	THREONINE--TRNA-LIGASE-RXN-THR-tRNAs/THR/ATP/PROTON//Charged-THR-tRNAs/AMP/PPI.52	15000.000000	0.079412
BURPS668_1752	lpdA	RXN-9718	15000.000000	0.079412
BURPS668_2178	purA	ADENYLOSUCCINATE-SYNTHASE-RXN	15000.000000	0.079412
BURPS668_2189	hisS	HISTIDINE--TRNA-LIGASE-RXN-HIS-tRNAs/HIS/ATP/PROTON//Charged-HIS-tRNAs/AMP/PPI.52	15000.000000	0.079412
BURPS668_2426	lpxD	UDPHYDROXYMYRGLUCOSAMNACETYLTRANS-RXN-R-3-hydroxymyristoyl-ACPs/UDP-OHMYR-GLUCOSAMINE//OH-MYRISTOYL/ACP/PROTON.73	15000.000000	0.000000
BURPS668_2433	uppS	RXN-8999	14545.454545	0.000000
BURPS668_2610	lpdA	1.8.1.4-RXN	15000.000000	0.079412
BURPS668_2788	fabF	3-OXOACYL-ACP-SYNTH-RXN /3-OXOACYL-ACP-SYNTH-BASE-RXN /2.3.1.41-RXN / many other reactions	15000.000000	0.079412
BURPS668_3103	rfbA	DTDPGLUCOSEPP-RXN	15000.000000	0.079412
BURPS668_3328	tgt	QUEUOSINE-TRNA-RIBOSYLTRANSFERASE-RXN; RXN0-1321	0.000000	0.079412
BURPS668_3366	ruvB	3.1.22.4-RXN	15000.000000	0.079412
BURPS668_3464	aroQ	3-DEHYDROQUINATE-DEHYDRATASE-RXN	15000.000000	0.079412
BURPS668_3525	murG	RXN-11346, RXN-8976, NACGLCTRANS-RXN, RXN-11029	10000.000000	0.000000
BURPS668_3561	ung	RXN0-2584	15000.000000	0.079412

BURPS668_3668	murA	UDPNACETYLGLUCOSAMENOLPYRTRANS-RXN	15000.000000	0.079412
BURPS668_A1869	ileS	ISOLEUCINE--TRNA-LIGASE-RXN	15000.000000	0.079412
BURPS668_A2053	acc	BIOTIN-CARBOXYL-RXN	15000.000000	0.079412
BURPS668_A2451	leuB	RXN-13158; 3-ISOPROPYLMALDEHYDROG-RXN	0.000000	0.079412
BURPS668_A2546	polA	DNA-DIRECTED-DNA-POLYMERASE-RXN	15000.000000	0.079412
BURPS668_A3190	lpdA	1.8.1.4-RXN/RXN0-1132/RXN-8629	15000.000000	0.079412

The overall biomass fluxes were different in the two models. The unconstrained model had a much greater total biomass flux than the LB media model. This is likely because the unconstrained model included more nutrient inputs than the LB media model.

4. Discussion

4.1 Links between metabolism and virulence

In order to colonize the host, establish an infection, and proliferate, pathogens employ various strategies, often involving links between metabolic pathways and virulence genes. Although current knowledge regarding the connections between metabolism and virulence is limited [60], this topic is becoming an increasing focus for host-pathogen studies. Some general links between metabolism and virulence include regulatory connections between specific metabolites and virulence gene expression [61-65], metabolic requirements for adaptation of the pathogen to the host niche [59,60,66,67], and carbon catabolite repression [68]. More detailed information on the topic of metabolism and virulence can be found in reviews [59,60,66,67,69-74].

Inside host cells, the survival of pathogenic bacteria depends on their acquisition of nutrients and carbon sources, such as carbohydrates, lipids, glycolipids, dicarboxylic acids and amino acids, from their host environment [59,60,66,67,71,75]. Preferred carbon sources vary among intracellular pathogens, and the types of nutrients available in the host cell cytosol may determine the cell-type specificities of different intracellular pathogens [76]. For example, many bacteria prefer hexoses, like glucose, as sources of carbon and energy. These sugars are catabolized through glycolysis, the pentose phosphate and Entner-Doudoroff pathways [75]. Some bacteria lack the glycolysis pathway and preferentially metabolize glucose via the Entner-Doudoroff pathway [77], while others lack both glycolysis and Entner-Doudoroff pathways and live on pyruvate that they obtain from the host cell cytosol [78].

4.2 Metabolic potential of B. pseudomallei MSHR668

We previously reported that *B. pseudomallei* MSHR668, K96243 and 1106a have abundant capabilities to metabolize hexoses, including the complete sets of genes encoding the glycolysis, pentose phosphate cycle, and Entner-Doudoroff pathways. They also have several pathways for metabolism of pyruvate to acetyl-CoA, acetate and ethanol [37]. In general, *B. pseudomallei* as a species has a very diverse set of metabolic capabilities, likely a reflection of its ability to live both in the natural environment and in hosts.

The metabolic power of *B. pseudomallei* has been targeted in mutation studies to address the roles of various metabolic genes in virulence. Mutation of various metabolic genes that affect cell growth results in attenuation of *B. pseudomallei* virulence; these genes include

315 phosphoribosylformylglycinamidine cyclo-ligase (*purM*) [79], aspartate-ß-semialdehyde
316 dehydrogenase (*asd*) [80], acetolactate synthase (*ilvI*) [21], dehydroquinate synthase (*aroB*) [20],
317 chorismate synthase (*aroC*) [17], phosphoserine aminotransferase (*serC*) [81],
318 phosphoribosylglycinamide formyltransferase 1 (*purN*) and phosphoribosylformylglycinamide
319 cyclo-ligase (*purM*) [18], two phospholipase C enzymes [82], disulfide oxidoreductase (*dsbA*) [83].
320 Targeted mutation of *purM*, which encodes aminoimidazole ribotide, a precursor of de novo adenine
321 and thiamine biosynthesis, predictably causes a deficiency in adenine and thiamine biosynthesis [79].
322 Aspartate-ß-semialdehyde dehydrogenase (*asd)* mutants cannot synthesize diaminopimelate for cell
323 wall biosynthesis [80], while acetolactate synthase (*ilvI)* mutants cannot synthesize the branched
324 chain amino acids isoleucine, valine, and leucine [21]. Dehydroquinate synthase (*aroB)* mutants are
325 defective in the shikimate pathway for chorismate biosynthesis, and addition of the aromatic
326 compounds tyrosine, tryptophan, phenylalanine, PABA, and 2,3-dihydroxybenzoate is required to
327 restore the growth in minimal medium [20]. Chorismate synthase (*aroC)* mutants are also defective
328 in aromatic compound synthesis and cannot grow without the addition of aromatic compounds to
329 the media [17]. Phosphoserine aminotransferase (*serC*) mutants are defective in serine and pyridoxal
330 5-phosphate biosynthesis and require minimal medium supplemented with serine for normal growth
331 [81].

332 *4.3 Vaccine studies*

333 Using live attenuated bacteria as vaccines can be effective in preventing disease, as attenuated
334 bacteria may still be able to replicate in the host and may contain immune-stimulatory epitopes that
335 are not found in subunit or heat-inactivated vaccines [84]. Many of the *B. pseudomallei* mutants
336 described above have already been tried as attenuated vaccines with mixed results. Vaccination with
337 the attenuated *asd* mutant protected BALB/c mice against acute melioidosis, but did not protect
338 against chronic melioidosis [80]. Vaccination with the attenuated *ilvI* mutant of *B. pseudomallei*
339 protected BALB/c mice against a challenge with a virulent strain [21]. In mice vaccinated with the
340 *aroB* mutant, the time to death following challenge with the virulent K96243 strain was a bit longer
341 than in unvaccinated mice, but all mice eventually died [20]. The *aroC* mutant was unable to persist
342 in vaccinated BALB/c mice long enough to elicit protective immunity, however C57BL/6 mice were
343 protected against challenge with a virulent strain [17]. Intraperitoneal vaccination of BALB/c mice
344 with a *serC* mutant resulted in higher levels of survival after challenge with K96243 virulent strain
345 [81]. While immunization of mice with attenuated *B. pseudomallei* mutants has resulted in the
346 induction of protective immunity in some cases, sterile immunity was rarely reported (reviewed by
347 [85]). Also, the live attenuated vaccine model may not be the best solution for the prevention of
348 melioidosis, because an attenuated mutant might revert to virulence, and might also establish a latent
349 infection [85].

350 *4.4 Identification of antimicrobial therapeutics*

351 An alternative avenue to combat melioidosis is through the development of novel antimicrobial
352 therapeutics. Regardless of the specific metabolic capabilities possessed by a pathogen, essential
353 nutrient acquisition and utilization mechanisms are proving to be good potential therapeutic targets,
354 as inhibition of these targets might deprive the pathogen of needed substrates for growth and
355 replication inside host cells [31]. There are currently 699 *B. pseudomallei* genomes available at the
356 National Center for Biotechnology Information (NCBI, http://www.ncbi.nlm.nih.gov/genome/476).
357 While some of these entries represent re-annotations of previous submissions, and some genomes
358 represent colony morphology variants of the same strain, an impressive number of individual
359 genomes are available to use with computational approaches to identify new therapeutic targets.
360 With this large number of available genomes, a core genome approach [86,87] could be used to
361 identify potential metabolic enzyme targets that are present in all sequenced *B. pseudomallei* genomes.
362 *In silico* methods for the identification of therapeutic targets in bacterial pathogens include
363 comparative genomics-based approaches, such as identification of essential genes specific to the

pathogen, and techniques based on metabolic pathway analysis and metabolic network modeling. The more robust approaches use a combination of comparative genomics and metabolic pathway analysis. These approaches have been used to identify essential gene targets in *Mycoplasma genitalium* [88] and *Mycobacterium ulcerans* [89]. Another method, subtractive target identification, involves identification of enzymes in the metabolic pathways of the pathogen, and comparing them to human proteins to identify pathogen enzymes that are not found in human. A list of likely targets is compiled by focusing on enzymes in pathways that are usually essential for pathogen growth and survival, like lipid metabolism, carbohydrate metabolism, amino acid metabolism, energy metabolism, vitamin and cofactor biosynthetic pathways and nucleotide metabolism. This approach has been used to identify putative targets in *M. tuberculosis* [90], MRSA [91-93], as well as a collection of other bacterial pathogens [94].

Methods for therapeutic target discovery based on metabolic pathway analysis and metabolic network modeling have become very popular in the last ten years. Numerous studies have identified candidate drug targets in various bacterial [27,34,95-106], fungal [106] and protosoan [31,106-109] pathogens using a variety of methods to analyze metabolic pathways and networks. One method employs chokepoint analysis to identify metabolic enzymes that are critical to the pathogen, because they uniquely consume and/or produce certain metabolites. Chokepoint analysis has been used to identify candidate metabolic enzyme targets in various pathogen genomes [27,31,34,99,107,108,110,111]. However, no studies to date have used this approach to identify potential drug targets in *B. pseudomallei* metabolic networks.

4.4.1 Identification of metabolic chokepoints

For this study, metabolic chokepoints were identified in the curated *B. pseudomallei* MSHR668 metabolic network using the Pathway Tools software [35]. Table 3 lists the chokepoint enzymes identified in the metabolic networks of *B. pseudomallei* MSHR668 and K96243. Twenty-four of the *B. pseudomallei* chokepoints were not indicated as human targets in DrugBank, and therefore represented good candidate therapeutic targets against melioidosis. Six of the chokepoints in Table 3 were aminoacyl-tRNA synthetases, which are likely good targets as they are critical enzymes involved in protein translation. These chokepoints included aspartyl-, threonyl-, histidyl-, valyl- and isoleucyl-tRNA synthetase (2 copies). Aspartyl-tRNA synthase (*aspS*) is an essential gene target in *M. tuberculosis* [112]. Threonyl-tRNA synthetase (*thrS*) inhibitors have been identified [113] and shown to have anti-malarial activity against *Plasmodium falciparum* [114]. Isoleucyl-tRNA synthetase (*ileS*) is a well-documented bacterial target [115-117]. The antimicrobial drug, mupirocin (pseudomonic acid), selectively inhibits bacterial isoleucyl-tRNA synthetase without inhibiting its human homolog [114]. However, resistance is seen in bacteria that possess an isoleucyl-tRNA synthetase that is similar to eukaryotic versions [118]. Histidyl-tRNA synthetase (*hisS*) has been explored as a target in *Trypanosoma cruzi* [119]. The chokepoint enzyme queuine tRNA-ribosyltransferase (*tgt*) incorporates the wobble base queuine into tRNA, and is also a target in *Zymomonas mobilis* and *Shigella* [120,121]

Several *B. pseudomallei* chokepoint enzymes are likely involved in DNA-related processes. Two of these enzymes, encoded by the *recA* and *dnaQ* genes, are involved in the SOS pathway [122], which mediates the bacterial response to DNA damage. Activation of the SOS response by ciprofloxacin induces mutations, which can lead to fluoriquinolone resistance [123]. The RecA protein is a target for antibacterial drug discovery in *M. tuberculosis* [124] and *Mycoplasma hyopneumoniae* [96], and has been proposed as a specific target for reducing the evolution of antimicrobial resistance [125]. The chokepoint enzyme deoxyuridine 5'-triphosphate nucleotidohydrolase (dUTPase) prevents incorporation of uracil into DNA and is important for DNA integrity [126]. dUTPase is a potential antimalarial drug target against *P. falciparum* [127,128]. Holliday junction DNA helicase (*ruvB*) participates in homologous recombination and repair of replication forks, and is therefore essential for bacterial growth. Holliday junction processing components were previously identified as targets for antimicrobials in *E. coli* [129] and *Neisseria gonorrhoeae* [130]. The chokepoint enzyme uracil-DNA glycosylase (*ung*) has a role in uracil excision repair, and is a candidate anti-malarial drug target [131], as well as a potential target to control growth of GC-rich bacteria such as *Pseudomonas aeruginosa* and

Mycobacterium smegmatis [132]. DNA polymerase I was identified as a chokepoint in *B. pseudomallei*. Putative inhibitors of DNA polymerase I (*polA*), and subsequently DNA synthesis, have been explored as possible antimicrobials [133,134].

Some chokepoint enzymes in *B. pseudomallei* have annotated functions in the biosynthesis of cell wall components. One of these, UDP-3-O-[3-hydroxymyristoyl] glucosamine N-acyltransferase (*lpxD*), catalyzes the third step in the lipid A biosynthesis pathway [135]. The lipid A component of bacterial LPS is of particular interest because it is essential for cell viability and is highly conserved [136]. This pathway is a target for new antibacterial therapeutics in *Escherichia coli* [137]. Another chokepoint involved in cell wall synthesis is undecaprenyl diphosphate synthase (*uppS*), which catalyzes the synthesis of a polyisoprenoid essential for both peptidoglycan and cell wall teichoic acid synthesis. UppS is a critical enzyme required for bacterial survival, and is an antibacterial target in *Staphylococcus aureus* [138], *Bacteroides fragilis*, *Vibrio vulnificus*, *E. coli* [139] and *H. pylori* [140]. Several classes of compounds that inhibit UppS function have been discovered [138,141,142]. Two additional *B. pseudomallei* chokepoints, undecaprenyldiphospho-muramoylpentapeptide beta-N-acetylglucosaminyltransferase (*murG*), and UDP-N-acetylglucosamine 1-carboxyvinyltransferase (*murA*) are likely involved in peptidoglycan biosynthesis. MurG is the target of the antibiotic ramoplanin in *Staphylococcus aureus* [143]. Other potential inhibitors of MurG have been identified by high throughput screening [144]. A small molecule inhibitor of MurG that augments the activity of β-lactams against methicillin-resistant *Staphylococcus aureus* was recently identified [145]. MurA has been a popular target for the design of novel antibiotics, and several inhibitors of MurA have been identified that are active against various bacterial species [91,146-151]. The chokepoint enzyme glucose-1-phosphate thymidylyltransferase (*rfbA*/*rmlA*), involved in O antigen biosynthesis, is also a target in *Streptococcus pneumoniae* [152] and *Pseudomonas aeruginosa* [153].

The rest of the chokepoint enzymes in Table 3 are components of various biosynthesis pathways. These enzymes include argininosuccinate synthase (*argG*), which catalyzes the second to last step in L-arginine biosynthesis, and is associated with pathogenesis in the parasite *Leishmania donovani* [154], *Streptococcus pneumoniae* [155], and *B. cenocepacia* [156]. The chokepoint enzyme 3-isopropylmalate dehydrogenase (*leuB*) is the third enzyme specific to leucine biosynthesis in microorganisms [157], and has been investigated as an antibacterial target in *M. tuberculosis* [158]. The *B. pseudomallei* chokepoint dihydroneopterin aldolase (*folB*) is part of the tetrahydrofolate biosynthesis process, and is essential for growth and biomass production in *Acinetobacter baylyi*, *Bacillus anthracis*, *Francisella tularensis*, *F. tularensis* subsp. novicida strain U112, *Mycobacterium tuberculosis*, *Helicobacter pylori*, *Pseudomonas aeruginosa*, *Salmonella enterica* serovar Typhi and *Yersinia pestis* [95]. Three of the chokepoint genes identified in *B. pseudomallei* encoded lipoamide dehydrogenase, a component of the pyruvate dehydrogenase complex, which converts pyruvate to acetyl-CoA as part of central metabolism [159]. Lipoamide dehydrogenase is also a target in *M. tuberculosis*, where deletion drastically impaired the pathogen's ability to establish infection in the mouse [160]. The mycobacterial version has only 36% identity with the human homolog. Lipoamide dehydrogenase is a target of drugs against trypanosomal infections [161]. Adenylosuccinate synthetase (*purA*) is also a chokepoint enzyme and potential therapeutic target that is involved in purine salvage in *Leishmania donovani* [162]. Chokepoint enzyme 3-dehydroquinate dehydratase (*aroQ*) is a component of the shikimate pathway for chorismate biosynthesis and is a target of known inhibitors in *M. tuberculosis*, *Enterococcus faecalis* and *Streptomyces coelicolor* [163-167].

The *B. pseudomallei* chokepoint enzyme 3-oxoacyl-ACP synthase (*fabF*), involved in fatty acid synthesis, is already an antibacterial target in *E. coli*, and a specific inhibitor, cerulenin, has been identified [168,169]. Another fatty acid synthesis chokepoint enzyme in *B. pseudomallei* was a biotin-dependent acetyl-CoA carbosylase. Biotin dependent carboxylases comprise a large group of enzymes that participate in a variety of cellular processes, including fatty acid metabolism, amino acid metabolism, carbohydrate metabolism, polyketide biosynthesis, urea utilization, etc. (reviewed by [170]). Acetyl-CoA carboxylase is comprised of two enzymes, biotin carboxylase and carboxyltransferase, and catalyzes the first committed step in fatty acid synthesis [171]. Acetyl-CoA carboxylase is an antimicrobial target in *M. tuberculosis* [172], *E. coli* [173,174], other bacteria and most

467 living organisms (reviewed by [175]). All of the chokepoints in Table 3 are essential genes in *B.*
468 *pseudomallei* MSHR668 and K96243, as determined by blasting the chokepoint enzyme sequences
469 against essential gene sequences in the Database of Essential Genes [176] and by comparing to the list
470 of essential genes previously identified in K96243 [177].
471 To determine if *B. pseudomallei* deletion mutants were available for each of the chokepoints in
472 Table 3, searches of the internet, PubMed, and the Burkholderia Genome Database
473 (http://burkholderia.com) were performed. Based on these searches, none of the chokepoint enzymes
474 in Table 3 had a mutant available; however, a *B. cenocepacia argG* mutant has attenuated virulence
475 [178], and *recA* mutants have been identified in *B. cepacia* [179].
476 Additional metabolic enzymes, not identified as chokepoints in this study, and pathways critical
477 for bacterial growth and survival have been mentioned with respect to target identification. These
478 include anaplerotic pathways that turned on by limiting carbon sources [180], the glyxoalate shunt
479 enzyme isocitrate lyase [16,181,182], involved in the metabolism of fatty acids [15,181], enoyl-ACP
480 reductase (FabI) in the type II fatty acid biosynthesis pathway [183], and alanine racemase [23].

481 4.4.2 Flux balance analysis

482 To gain an understanding of the metabolic processes in *B. pseudomallei* MSHR668 that are active
483 under different environmental conditions, and to test the effect of deletion of each chokepoint enzyme
484 on the growth of *B. pseudomallei in silico*, metabolic network models were constructed and FBA was
485 performed. The first FBA model, of the unconstrained network in MSHR668, included all possible
486 biomass compounds that could be produced, all nutrients that could be consumed, had no weights
487 imposed on the biomass metabolites and no constraints imposed on the nutrients. [Supplementary
488 material, S1_Final_unconstrained_model_inputs.pdf, S2_Final_unconstrained_model_solution.pdf].
489 This model likely represents the metabolic potential of *B. pseudomallei* in a soil or water environment
490 where abundant carbon and nitrogen sources are available. To mimic the conditions that *B.*
491 *pseudomallei* experiences in culture, a separate model was constructed that provided only the
492 nutrients present in LB media plus glycerol [43]. Constraints were included on some of the nutrients
493 in this model (ADP, Pi, proton and glycerol). [Supplementary material,
494 S3_Final_LB_model_inputs.pdf, S4_Final_LB_model_solution.pdf]. A third model was attempted, to
495 mimic infection conditions using only the nutrients present in the host cell cytosol. However, no
496 comprehensive studies have identified a complete list of host cell nutrients that are available to *B.*
497 *pseudomallei* during infection. Also, the specific carbon requirements of *B. pseudomallei* in either
498 human macrophages or amoebae have not been determined. After trying to compile a list of nutrients
499 that mimic the content of the host cytosol, from the literature and from gene expression studies of *B.*
500 *pseudomallei* during infection, this model did not produce a solution so it was abandoned. However,
501 the LB media model contained a similar set of nutrients to those used by the intracellular pathogen
502 *L. pneumophila* [47,48,50],. so it may in fact be somewhat representative of infection conditions.
503 *In silico* knockout experiments were performed, where each chokepoint enzyme was knocked
504 out, one at a time, to assess the effect on the total flux through the unconstrained and LB media
505 models. Five chokepoint enzymes, when knocked out, had an effect on the models (Table 4).
506 Specifically, knocking out BURPS668_3328 (*tgt*) and BURPS668_A2451 (*leuB*), eliminated the biomass
507 flux in the unconstrained model, while knockout of BURPS668_2426 (*lpxD*), BURPS668_2433 (*uppS*),
508 and BURPS668_3525 (*murG*) eliminated the biomass flux in the LB media model. Knockout of
509 BURPS668_2433 (*uppS*), and BURPS668_3525 (*murG*) decreased the biomass flux in the unconstrained
510 model, but did not eliminate it. The metabolic pathways that these enzymes belong to are shown in
511 Figure 2.

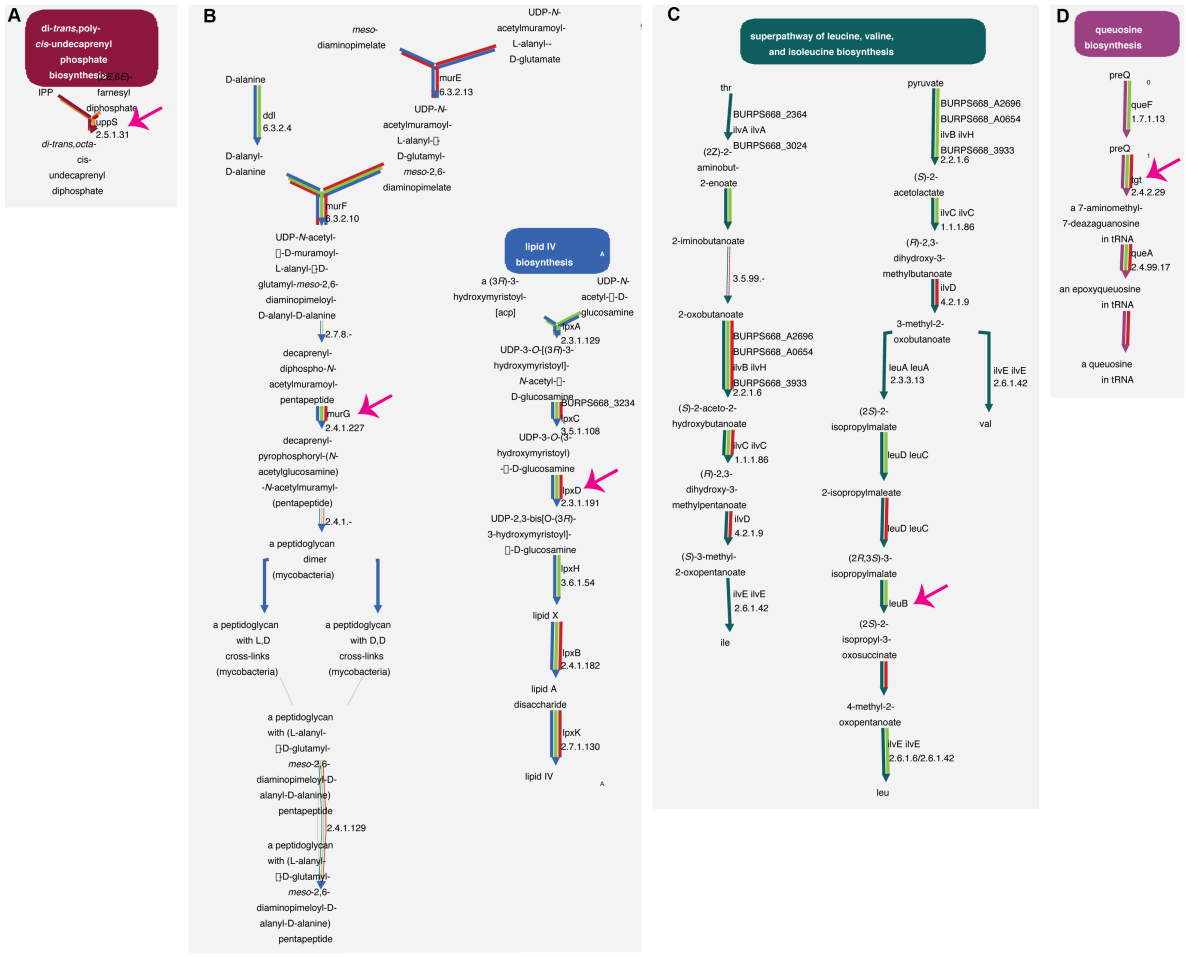

Figure 2. Metabolic pathways in *B. pseudomallei* MSHR668 that show reduced flux when chokepoint enzymes (indicated by pink arrows) are deleted. A. The mono-trans, poly-cis decaprenyl phosphate biosynthesis pathway that contains the chokepoint enzyme undecaprenyl diphosphate synthase (*uppS*). B. The two chokepoints UDP-N-acetylglucosamine--N-acetylmuramyl-(pentapeptide) pyrophosphoryl-decaprenol N-acetylglucosamine transferase (*murG*) and UDP-3-O-(R-3-hydroxymyristoyl)-glucosamine N-acyltransferase (*lpxD*), involved in peptidoglycan and lipid A biosynthesis, respectively. C. The chokepoint enzyme tRNA-guanine transglycosylase (*tgt*), involved in queosine biosynthesis. D. The 3-isopropylmalate dehydrogenase (*leuB*) chokepoint enzyme performs the third step in leucine biosynthesis. *In silico* deletion of UDP-3-O-(R-3-hydroxymyristoyl)-glucosamine N-acyltransferase (*lpxD*) reduced flux through the *B. pseudomallei* metabolic network in the LB media model, deletion of undecaprenyl diphosphate synthase (*uppS*) reduced flux through both unconstrained and LB media models, and deletion of tRNA-guanine transglycosylase (*tgt*) and 3-isopropylmalate dehydrogenase (*leuB*) reduced flux in the unconstrained model. These pathways were rendered by the Cellular Overview feature of Pathway Tools.

In terms of carbon sources, glucose was utilized as a nutrient in the unconstrained model of *B. pseudomallei* MSHR668. However, when glycerol was replaced by glucose in the LB media model, no FBA solution was found [data not shown]. This was a somewhat unexpected result, as *B. pseudomallei* can utilize glucose as a carbon source in culture [184]. One possible explanation for this result is that additional nutrients required for glucose utilization were missing from the input nutrients list. Co-metabolism of more than one carbon substrate is a metabolic strategy employed by intracellular bacteria replicating inside host cells to provide carbon for energy and biosynthesis [59]. For example, *Listeria monocytogenes* can use both glycerol and lactate as carbon sources, [57,185-187]. It has been suggested that during infection by *Listeria*, the host cell may not contain enough glucose to activate bacterial PTS glucose transporters, so alternative carbon sources are important for survival and virulence of the pathogen [57]. *M. tuberculosis* also relies on glycerol and fatty acids as carbon sources

in the macrophage environment [188] As the unconstrained *B. pseudomallei* model included a much longer list of nutrients than the LB model and also could use glucose as a nutrient, this could be the case. Another explanation for glucose not being utilized by the LB media model is that intracellular bacteria seem to prefer other substrates over glucose during infection [189], and glycerol may be a major carbon source for intracellular bacteria during infection [189,190]. This may also be the situation for *B. pseudomallei* inside host cells. Glycerol feeds into the second half of the glycolysis/gluconeogenesis pathway through its conversion to dihydroxyacetone phosphate [www.metacyc.org; [191]], bypassing the first four steps of glycolysis. We previously determined that the *B. pseudomallei* MSHR668 genome has the full set of genes to perform this conversion [37]. Two studies of *L. monocytogenes* infection support the idea that intracellular pathogens generally may use glycerol rather than glucose as a main carbon source while inside host cells. Transcription profiles of *L. monocytogenes* grown in mouse macrophages showed reduced expression of genes encoding some of the enzymes involved in glycolysis, in particular phosphoglucose isomerase (*pgi*), which converts glucose-6-phosphate into fructose-6-phosphate, and the five steps involved in the conversion of glyceraldehyde-3-phosphate to pyruvate [189]. Similar transcription profiles were seen during *L. monocytogenes* infection of Caco-2 epithelial cells [192]. Both studies showed increased expression of genes involved in the uptake and utilization of glycerol [189,192]: these genes were *glpF*, *glpK*, *glpD* and *dhaK*.

To date, no study has determined precisely which carbon substrates are utilized by *B. pseudomallei* during infection of host cells. In addition to glycerol, there is evidence that *B. pseudomallei* may utilize aromatic carbon compounds such as benzoate and phenylacetic acid as carbon sources for intracellular survival [53]. One study showed that in *B. pseudomallei* 1026b, glycolytic pathway and TCA cycle genes were down-regulated during infection of hamster [193], supporting the idea that *B. pseudomallei* may prefer carbon sources other than glucose while inside host cells. Other studies examined genes induced by hypoxia, which is a condition present in infected macrophages [194] and changes in *B. pseudomallei* gene expression during infection of rat lungs {van Schaik, 2008 #194.

Complicating the situation even more, the complete nutrient content of a representative mammalian host cell cytosol has not been determined yet, so a consensus set of nutrients present in the cytosol of different host cell types is still out of reach {Eisenreich, 2013 #40}. This is largely due to the challenges in designing appropriate infection models and robust analytical approaches to measure metabolic changes occurring in host cells during infection. Because of these limitations on both the pathogen and host sides, it is difficult to predict which carbon sources pathogens can use to grow inside host cells. While we don't know the exact biochemical composition of a mammalian cell cytosol, we do know some details about mammalian cells in general. For example, the cytosol of a typical cell has low magnesium, sodium and calcium concentrations, and a high potassium concentration at neutral pH [195]. In addition, mammalian cells contain small amounts of amino acids, plus significant amounts of TCA cycle intermediates [196,197]. Once inside host cells, intracellular bacteria may stimulate host cell responses to produce needed nutrients [190]. However, host-pathogen interactions during infection are complicated, as some host defense responses are aimed at inhibiting pathogen survival and proliferation, for instance by decreasing metabolic activities that provide nutrients to the pathogen [180].

5. Conclusions

This work is the first to use genome scale metabolic modeling to address *B. pseudomallei* metabolism as a source of new drug targets. While identifying the nutrients available to *B. pseudomallei* inside host cells was difficult, the effort described here identified a set of twenty-six chokepoint enzyme drug targets; *in silico* deletion of five of these target enzymes reduced the total biomass flux through the *B. pseudomallei* metabolic network. While a genome-based approach like this can streamline the initial steps of antibacterial target identification, the true utility of this process will be demonstrated when the targets are experimentally verified by performing knockout experiments in culture, followed by efficacy testing of candidate drugs in culture and in animal models of infection.

Supplementary Materials: The following are available online at www.mdpi.com/link, S1_Final_unconstrained_model_inputs.pdf,S2_Final_unconstrained_model_solution.pdf, S3_Final_LB_model_inputs.pdf, S4_Final_LB_model_solution.pdf, S5_Nutrients_infection_model.pdf

Acknowledgments: This project was supported by the Defense Threat Reduction Agency (JSTO-CBD Proposal # CBCALL12-IS1-1-0283).

Conflicts of Interest: The author declares no conflict of interest. The founding sponsors had no role in the design of the study; in the collection, analyses, or interpretation of data; in the writing of the manuscript, and in the decision to publish the results.

References

1. White, N.J. Melioidosis. *Lancet* **2003**, *361*, 1715-1722.
2. Currie, B.J. Melioidosis: An important cause of pneumonia in residents of and travellers returned from endemic regions. *Eur Respir J* **2003**, *22*, 542-550.
3. Schweizer, H.P. Mechanisms of antibiotic resistance in *Burkholderia pseudomallei*: Implications for treatment of melioidosis. *Future Microbiol.* **2012**, *7*, 1389-1399.
4. Dance, D. Treatment and prophylaxis of melioidosis. *Int J Antimicrob Agents.* **2014**, *43*, 310-318.
5. Mays, E.E.; Ricketts, E.A. Melioidosis: Recrudescence associated with bronchogenic carcinoma twenty-six years following initial geographic exposure. *Chest* **1975**, *68*.
6. Thibault, F.M.; Hernandez, E.; Vidal, D.R.; Girardet, M.; Cavallo, J.D. Antibiotic susceptibility of 65 isolates of *Burkholderia pseudomallei* and *Burkholderia mallei* to 35 antimicrobial agents. *J. Antimicrob. Chemother.* **2004**, *54*, 1134-1138.
7. Jenney, A.W.; Lum, G.; Fisher, D.A.; Currie, B.J. Antibiotic susceptibility of *Burkholderia pseudomallei* from tropical northern australia and implications for therapy of melioidosis. *Int. J. Antimicrob. Agents* **2001**, *17*, 109-113.
8. Dance, D.A.; Wuthiekanun, V.; Chaowagul, W.; White, N.J. The antimicrobial susceptibility of *Pseudomonas pseudomallei*. Emergence of resistance in vitro and during treatment. *J Antimicrob Chemother.* **1989**, *24*, 295-309.
9. Galperin, M.Y.; Koonin, E.V. Searching for drug targets in microbial genomes. *Curr Opin Biotechnol.* **1999**, *10*, 571-578.
10. Oberhardt, M.A.; Yizhak, K.; Ruppin, E. Metabolically re-modeling the drug pipeline. *Curr Opin Pharmacol.* **2013**, *13*, 778-785.
11. Silver, L.L. Challenges of antibacterial discovery. *Clin Microbiol Rev.* **2011**, *24*, 71-109.
12. Cummings, J.E.; Kingry, L.C.; Rholl, D.A.; Schweizer, H.P.; Tonge, P.J.; Slayden, R.A. The *Burkholderia pseudomallei* enoyl-acyl carrier protein reductase fabi1 is essential for in vivo growth and is the target of a novel chemotherapeutic with efficacy. *Antimicrob Agents Chemother.* **2014**, *58*, 931-935.
13. Lu, H.; Tonge, P.J. Inhibitors of fabi, an enzyme drug target in the bacterial fatty acid biosynthesis pathway. *Acc Chem Res.* **2008**, *41*, 11-20.
14. Tong, L.; Harwood, H.J.J. Acetyl-coenzyme a carboxylases: Versatile targets for drug discovery. *J Cell Biochem* **2006**, *99*, 1478-1488.
15. Muñoz-Elías, E.J.; McKinney, J.D. *Mycobacterium tuberculosis* isocitrate lyases 1 and 2 are jointly required for in vivo growth and virulence. *Nat Med.* **2005**, *11*, 638-644.

16. van Schaik, E.J.; Tom, M.; Woods, D.E. *Burkholderia pseudomallei* isocitrate lyase is a persistence factor in pulmonary melioidosis: Implications for the development of isocitrate lyase inhibitors as novel antimicrobials. *Infect Immun.* **2009**, *77*, 4275-4283.
17. Srilunchang, T.; Proungvitaya, T.; Wongratanacheewin, S.; Strugnell, R.; Homchampa, P. Construction and characterization of an unmarked aroc deletion mutant of *Burkholderia pseudomallei* strain a2. *Southeast Asian J Trop Med Public Health* **2009**, *40*, 123-130.
18. Breitbach, K.; Köhler, J.; Steinmetz, I. Induction of protective immunity against *Burkholderia pseudomallei* using attenuated mutants with defects in the intracellular life cycle. *Trans R Soc Trop Med Hyg* **2008**, *102 Suppl 1*, S89-94.
19. Pilatz, S.; Breitbach, K.; Hein, N.; Fehlhaber, B.; Schulze, J.; Brenneke, B.; Eberl, L.; Steinmetz, I. Identification of *Burkholderia pseudomallei* genes required for the intracellular life cycle and in vivo virulence. *Infect Immun* **2006**, *74*, 3576-3586.
20. Cuccui, J.; Easton, A.; Chu, K.K.; Bancroft, G.J.; Oyston, P.C.; Titball, R.W.; Wren, B.W. Development of signature-tagged mutagenesis in *Burkholderia pseudomallei* to identify genes important in survival and pathogenesis. *Infect Immun* **2007**, *75*, 1186-1195.
21. Atkins, T.; Prior, R.G.; Mack, K.; Russell, P.; Nelson, M.; Oyston, P.C.; Dougan, G.; Titball, R.W. A mutant of *Burkholderia pseudomallei*, auxotrophic in the branched chain amino acid biosynthetic pathway, is attenuated and protective in a murine model of melioidosis. *Infect Immun* **2002**, *70*, 5290-5294.
22. Levine, H.B.; Maurer, R.L. Immunization with an induced avirulent auxotrophic mutant of *Pseudomonas pseudomallei*. *J Immunol* **1958**, *81*, 433-438.
23. Zajdowicz, S.L.; Jones-Carson, J.; Vazquez-Torres, A.; Jobling, M.G.; Gill, R.E.; Holmes, R.K. Alanine racemase mutants of *Burkholderia pseudomallei* and *Burkholderia mallei* and use of alanine racemase as a non-antibiotic-based selectable marker. *PLoS One* **2011**, *6*, e21523.
24. Vanaporn, M.; Wand, M.; Michell, S.L.; Sarkar-Tyson, M.; Ireland, P.; Goldman, S.; Kewcharoenwong, C.; Rinchai, D.; Lertmemongkolchai, G.; Titball, R.W. Superoxide dismutase c is required for intracellular survival and virulence of *Burkholderia pseudomallei*. *Microbiology* **2011**, *157*, 2392-2400.
25. Lee, H.S.; Gu, F.; Ching, S.M.; Lam, Y.; Chua, K.L. Cdpa is a *Burkholderia pseudomallei* cyclic di-gmp phosphodiesterase involved in autoaggregation, flagellum synthesis, motility, biofilm formation, cell invasion, and cytotoxicity. *Infect Immun* **2010**, *78*, 1832-1840.
26. McPhillie, M.J.; Cain, R.M.; Narramore, S.; Fishwick, C.W.; Simmons, K.J. Computational methods to identify new antibacterial targets. *Chem Biol Drug Des.* **2015**, *85*, 22-29.
27. Chung, B.K.; Dick, T.; Lee, D.Y. In silico analyses for the discovery of tuberculosis drug targets. *J Antimicrob Chemother.* **2013**, *68*, 2701-2709.
28. Mobegi, F.M.; van Hijum, S.A.; Burghout, P.; Bootsma, H.J.; de Vries, S.P.; van der Gaast-de Jongh, C.E.; Simonetti, E.; Langereis, J.D.; Hermans, P.W.; de Jonge, M.I., *et al.* From microbial gene essentiality to novel antimicrobial drug targets. *BMC Genomics* **2014**, *15*, 958.
29. Hamilton, J.J.; Reed, J.L. Software platforms to facilitate reconstructing genome-scale metabolic networks. *Environ Microbiol.* **2014**, *16*, 49-59.
30. Thiele, I.; Palsson, B.Ø. A protocol for generating a high-quality genome-scale metabolic reconstruction. *Nat. Protoc.* **2010**, *5*, 93-121.

31. Yeh, I.; Hanekamp, T.; Tsoka, S.; Karp, P.D.; Altman, R.B. Computational analysis of *Plasmodium falciparum* metabolism: Organizing genomic information to facilitate drug discovery. *Genome Res* **2004**, *14*, 917-924.
32. Duffield, M.; Cooper, I.; McAlister, E.; Bayliss, M.; Ford, D.; Oyston, P. Predicting conserved essential genes in bacteria: In silico identification of putative drug targets. *Mol Biosyst.* **2010**, *6*, 2482-2489.
33. Sakharkar, K.R.; Sakharkar, M.K.; Chow, V.T. A novel genomics approach for the identification of drug targets in pathogens, with special reference to *Pseudomonas aeruginosa*. *In Silico Biol.* **2004**, *4*, 355-360.
34. Singh, S.; Malik, B.K.; Sharma, D.K. Metabolic pathway analysis of *s. Pneumoniae*: An in silico approach towards drug-design. *J Bioinform Comput Biol* **2007**, *5*, 135-153.
35. Karp, P.D.; Paley, S.; Romero, P. The pathway tools software. *Bioinformatics* **2002**, *18 Suppl 1*, S225-S232.
36. Aziz, R.K.; Bartels, D.; Best, A.A.; DeJongh, M.; Disz, T.; Edwards, R.A.; Formsma, K.; Gerdes, S.; Glass, E.M.; Kubal, M., *et al.* The rast server: Rapid annotations using subsystems technology. *BMC Genomics* **2008**, *9*, 75.
37. Challacombe, J.F.; Stubben, C.J.; Klimko, C.P.; Welkos, S.L.; Kern, S.J.; Bozue, J.A.; Worsham, P.L.; Cote, C.K.; Wolfe, D.N. Interrogation of the *Burkholderia pseudomallei* genome to address differential virulence among isolates. *PLoS One* **2014**, *9*, e115951.
38. Karp, P.D.; Latendresse, M.; Caspi, R. The pathway tools pathway prediction algorithm. *Stand Genomic Sci* **2011**, *5*, 424-429.
39. Latendresse, M.; Krummenacker, M.; Trupp, M.; Karp, P.D. Construction and completion of flux balance models from pathway databases. *Bioinformatics* **2102**, *28*, 388-396.
40. Fraser, D.; Powell, R.E. The kinetics of trypsin digestion. *J Biol Chem.* **1950**, *187*, 803-820.
41. Bertani, G. Studies on lysogenesis. I. The mode of phage liberation by lysogenic *Escherichia coli*. *J Bacteriol.* **1951**, *62*, 293-300.
42. Grant, C.L.; Pramer, D. Minor element composition of yeast extract. *J Bacteriol.* **1962**, *84*, 869-870.
43. Oh, Y.K.; Palsson, B.O.; Park, S.M.; Schilling, C.H.; Mahadevan, R. Genome-scale reconstruction of metabolic network in *Bacillus subtilis* based on high-throughput phenotyping and gene essentiality data. *J Biol Chem.* **2007**, *282*, 28791-28799.
44. Zhang, R.; Lin, Y. Deg 5.0, a database of essential genes in both prokaryotes and eukaryotes. *Nucleic Acids Res.* **2009**, *37(Database issue)*, D455-458.
45. Wishart, D.S.; Knox, C.; Guo, A.C.; Cheng, D.; Shrivastava, S.; Tzur, D.; Gautam, B.; Hassanali, M. Drugbank: A knowledgebase for drugs, drug actions and drug targets. *Nucleic Acids Res.* **2008**, *36(Database issue)*, D901-906.
46. Shannon, P.; Markiel, A.; Ozier, O.; Baliga, N.S.; Wang, J.T.; Ramage, D.; Amin, N.; Schwikowski, B.; Ideker, T. Cytoscape: A software environment for integrated models of biomolecular interaction networks. *Genome Res* **2003**, *13*, 2498-2504.
47. Price, C.T.; Richards, A.M.; Abu Kwaik, Y. Nutrient generation and retrieval from the host cell cytosol by intra-vacuolar *Legionella pneumophila*. *Front Cell Infect Microbiol* **2014**, *4*, 111.
48. Price, C.T.; Abu Kwaik, Y. Amoebae and mammals deliver protein-rich atkins diet meals to *Legionella* cells. *Microbe* **2012**, *7*, 506-513.

49. Gao, L.Y.; Harb, O.S.; Abu Kwaik, Y. Utilization of similar mechanisms by *Legionella pneumophila* to parasitize two evolutionarily distant host cells, mammalian macrophages and protozoa. *Infect. Immun.* **1997**, *65*, 4738-4746.
50. Eylert, E.; Herrmann, V.; Jules, M.; Gillmaier, N.; Lautner, M.; Buchrieser, C.; Eisenreich, W.; Heuner, K. Isotopologue profiling of *Legionella pneumophila*: Role of serine and glucose as carbon substrates. *J Biol Chem.* **2010**, *285*, 22232-22243.
51. DeShazer, D. Genomic diversity of *Burkholderia pseudomallei* clinical isolates: Subtractive hybridization reveals a *Burkholderia mallei*-specific prophage in *B. pseudomallei* 1026b. *J. Bacteriol.* **2004**, *186*, 3938-3950.
52. Ooi, W.F.; Ong, C.; Nandi, T.; Kreisberg, J.F.; Chua, H.H.; Sun, G.; Chen, Y.; Mueller, C.; Conejero, L.; Eshaghi, M., *et al.* The condition-dependent transcriptional landscape of *Burkholderia pseudomallei*. *PLoS Genet.* **2013**, *9*, e1003795.
53. Chieng, S.; Carreto, L.; Nathan, S. *Burkholderia pseudomallei* transcriptional adaptation in macrophages. *BMC Genomics* **2012**, *13*, 328.
54. Eriksson, S.; Lucchini, S.; Thompson, A.; Rhen, M.; Hinton, J.C. Unravelling the biology of macrophage infection by gene expression profiling of intracellular *Salmonella enterica*. *Mol Microbiol* **2003**, *47*, 103-118.
55. Zdziarski, J.; Brzuszkiewicz, E.; Wullt, B.; Liesegang, H.; Biran, D.; Voigt, B.; Grönberg-Hernandez, J.; Ragnarsdottir, B.; Hecker, M.; Ron, E.Z., *et al.* Host imprints on bacterial genomes--rapid, divergent evolution in individual patients. *PLoS Pathog.* **2010**, *6*, e1001078.
56. Reniere, M.L.; Whiteley, A.T.; Hamilton, K.L.; John, S.M.; Lauer, P.; Brennan, R.G.; Portnoy, D.A. Glutathione activates virulence gene expression of an intracellular pathogen. *Nature* **2015**, *517*, 70-31.
57. Eylert, E.; Schär, J.; Mertins, S.; Stoll, R.; Bacher, A.; Goebel, W.; Eisenreich, W. Carbon metabolism of *Listeria monocytogenes* growing inside macrophages. *Mol Microbiol.* **2008**, *69*, 1008-1017.
58. Chico-Calero, I.; Suárez, M.; González-Zorn, B.; Scortti, M.; Slaghuis, J.; Goebel, W.; Vázquez-Boland, J.A.; Consortium, E.L.G. Hpt, a bacterial homolog of the microsomal glucose- 6-phosphate translocase, mediates rapid intracellular proliferation in *Listeria*. *Proc Natl Acad Sci U S A* **2002**, *99*, 431-436.
59. Eisenreich, W.; Dandekar, T.; Heesemann, J.; Goebel, W. Carbon metabolism of intracellular bacterial pathogens and possible links to virulence. *Nat Rev Microbiol* **2010**, *8*, 401-412.
60. Fuchs, T.M.; Eisenreich, W.; Heesemann, J.; Goebel, W. Metabolic adaptation of human pathogenic and related nonpathogenic bacteria to extra- and intracellular habitats. *FEMS Microbiol Rev.* **2012**, *36*, 435-462.
61. Gore, A.L.; Payne, S.M. Csra and cra influence *Shigella flexneri* pathogenesis. *Infect Immun.* **2010**, *78*, 4674-4682.
62. Litwin, C.M.; Calderwood, S.B. Role of iron in regulation of virulence genes. *Clin Microbiol Rev.* **1993**, *6*, 137-149.
63. Mellies, J.L.; Barron, A.M.; Carmona, A.M. Enteropathogenic and enterohemorrhagic *Escherichia coli* virulence gene regulation. *Infect Immun* **2007**, *75*, 4199-4210.

64. Njoroge, J.W.; Nguyen, Y.; Curtis, M.M.; Moreira, C.G.; Sperandio, V. Virulence meets metabolism: Cra and kdpe gene regulation in enterohemorrhagic *Escherichia coli*. *MBio* **2012**, *3*, e00280-00212.
65. Porcheron, G.; Dozois, C.M. Interplay between iron homeostasis and virulence: Fur and ryhb as major regulators of bacterial pathogenicity. *Vet Microbiol* **2015**, *179*, 2-14.
66. Ray, K.; Marteyn, B.; Sansonetti, P.J.; Tang, C.M. Life on the inside: The intracellular lifestyle of cytosolic bacteria. *Nat Rev Microbiol* **2009**, *7*, 333-340.
67. Rohmer, L.; Hocquet, D.; Miller, S.I. Are pathogenic bacteria just looking for food? Metabolism and microbial pathogenesis. *Trends Microbiol.* **2011**, *19*, 341-348.
68. Gorke, B.; Stulke, J. Carbon catabolite repression in bacteria: Many ways to make the most out of nutrients. *Nat Rev Microbiol* **2008**, *6*, 613-624.
69. Barel, M.; Charbit, A. *Francisella tularensis* intracellular survival: To eat or to die. *Microbes Infect* **2013**, *pii*, S1286-4579(1213)00206-00202.
70. Kwaik, Y.A. Nutrition-based evolution of intracellular pathogens. *Environmental Microbiology Reports* **2015**, *7*, 2-3.
71. Kwaik, Y.A.; Bumann, D. Microbial quest for food in vivo: 'Nutritional virulence' as an emerging paradigm. *Cell Microbiol.* **2013**, *15*, 882-890.
72. Meibom, K.L.; Charbit, A. *Francisella tularensi*s metabolism and its relation to virulence. *Front Microbiol.* **2010**, *1*, 140.
73. Olive, A.J.; Sassetti, C.M. Metabolic crosstalk between host and pathogen: Sensing, adapting and competing. *Nature Reviews Microbiology* **2016**, *14*, 221-234.
74. Santic, M.; Kwaik, Y.A. Nutritional virulence of *Francisella tularensis*. *Front Cell Infect Microbiol* **2013**, *3*, 112.
75. Muñoz-Elías, E.J.; McKinney, J.D. Carbon metabolism of intracellular bacteria. *Cell Microbiol.* **2006**, *8*, 10-22.
76. Brown, S.A.; Palmer, K.L.; Whiteley, M. Revisiting the host as a growth medium. *Nat Rev Microbiol.* **2008**, *6*, 657-666.
77. Fuhrer, T.; Fischer, E.; Sauer, U. Experimental identification and quantification of glucose metabolism in seven bacterial species. *J Bacteriol.* **2005**, *187*, 1581-1590.
78. Renesto, P.; Ogata, H.; Audic, S.; Claverie, J.M.; Raoult, D. Some lessons from *Rickettsia* genomics. *FEMS Microbiol Rev* **2005**, *29*, 99-117.
79. Propst, K.L.; Mima, T.; Choi, K.H.; Dow, S.W.; Schweizer, H.P. A *Burkholderia pseudomallei* deltapurm mutant is avirulent in immunocompetent and immunodeficient animals: Candidate strain for exclusion from select-agent lists. *Infect Immun* **2010**, *78*, 3136-3143.
80. Norris, M.H.; Propst, K.L.; Kang, Y.; Dow, S.W.; Schweizer, H.P.; Hoang, T.T. The *Burkholderia pseudomallei* δasd mutant exhibits attenuated intracellular infectivity and imparts protection against acute inhalation melioidosis in mice. *Infect Immun* **2011**, *79*, 4010-4018.
81. Rodrigues, F.; Sarkar-Tyson, M.; Harding, S.V.; Sim, S.H.; Chua, H.H.; Lin, C.H.; Han, X.; Karuturi, R.K.; Sung, K.; Yu, K., *et al.* Global map of growth-regulated gene expression in *Burkholderia pseudomallei*, the causative agent of melioidosis. *J Bacteriol* **2006**, *188*, 8178-8188.
82. Korbsrisate, S.; Tomaras, A.P.; Damnin, S.; Ckumdee, J.; Srinon, V.; Lengwehasatit, I.; Vasil, M.L.; Suparak, S. Characterization of two distinct phospholipase c enzymes from *Burkholderia pseudomallei*. *Microbiology* **2007**, *153*, 1907-1915.

83. Ireland, P.M.; McMahon, R.M.; Marshall, L.E.; Halili, M.; Furlong, E.; Tay, S.; Martin, J.L.; Sarkar-Tyson, M. Disarming *Burkholderia pseudomallei:* Structural and functional characterization of a disulfide oxidoreductase (DsbA) required for virulence in vivo. *Antioxid Redox Signal* **2014**, *20*, 606-617.

84. Drabner, B.; Guzmán, C.A. Elicitation of predictable immune responses by using live bacterial vectors. *Biomol Eng* **2001**, *17*, 75-82.

85. Peacock, S.J.; Limmathurotsakul, D.; Lubell, Y.; Koh, G.C.; White, L.J.; Day, N.P.; Titball, R.W. Melioidosis vaccines: A systematic review and appraisal of the potential to exploit biodefense vaccines for public health purposes. *PLoS Negl Trop Dis* **2012**, *6*, e1488.

86. Sim SH, Y.Y., Lin CH, Karuturi RKM, Wuthiekanun V, Tuanyok A. The core and accessory genomes of *Burkholderia pseudomallei*: Implications for human melioidosis. *PLoS Pathog* **2008**, *4*, e1000178.

87. Sahl, J.W.; Vazquez, A.J.; Hall, C.M.; Busch, J.D.; Tuanyok, A.; Mayo, M.; Schupp, J.M.; Lummis, M.; Pearson, T.; Shippy, K., *et al.* The effects of signal erosion and core genome reduction on the identification of diagnostic markers. *mBio* **2016**, *7*, e00846-00816.

88. Butt, A.M.; Tahir, S.; Nasrullah, I.; Idrees, M.; Lu, J.; Tong, Y. *Mycoplasma genitalium*: A comparative genomics study of metabolic pathways for the identification of drug and vaccine targets. *Infect Genet Evol* **2012**, *12*, 53-62.

89. Butt, A.M.; Nasrullah, I.; Tahir, S.; Tong, Y. Comparative genomics analysis of *Mycobacterium ulcerans* for the identification of putative essential genes and therapeutic candidates. *PLoS One* **2012**, *7*, e43080.

90. Anishetty, S.; Pulimi, M.; Pennathur, G. Potential drug targets in *Mycobacterium tuberculosis* through metabolic pathway analysis. *Comput Biol Chem* **2005**, *29*, 368-378.

91. Yadav, P.K.; Singh, G.; Singh, S.; Gautam, B.; Saad, E.I. Potential therapeutic drug target identification in community acquired-methicillin resistant *Staphylococcus aureus* (ca-mrsa) using computational analysis. *Bioinformation* **2012**, *8*, 664-672.

92. Uddin, R.; Saeed, K. Identification and characterization of potential drug targets by subtractive genome analyses of methicillin resistant *Staphylococcus aureus*. *Comput Biol Chem* **2014**, *48*, 55-63.

93. Uddin, R.; Saeed, K.; Khan, W.; Azam, S.S.; Wadood, A. Metabolic pathway analysis approach: Identification of novel therapeutic target against methicillin resistant *Staphylococcus aureus*. *Gene* **2015**, *556*, 213-226.

94. Barh, D.; Tiwari, S.; Jain, N.; Ali, A.; Santos, A.R.; Misra, A.N.; Azevedo, V.; Kumar, A. In silico subtractive genomics for target identification in human bacterial pathogens. *Drug Dev. Res.* **2011**, *72*, 162-177.

95. Ahn, Y.Y.; Lee, D.S.; Burd, H.; Blank, W.; Kapatral, V. Metabolic network analysis-based identification of antimicrobial drug targets in category a bioterrorism agents. *PLoS One* **2014**, *9*, e85195.

96. Damte, D.; Suh, J.W.; Lee, S.J.; Yohannes, S.B.; Hossain, M.A.; Park, S.C. Putative drug and vaccine target protein identification using comparative genomic analysis of kegg annotated metabolic pathways of *Mycoplasma hyopneumoniae*. *Genomics* **2013**, *102*, 47-56.

97. Fang, K.; Zhao, H.; Sun, C.; Lam, C.M.; Chang, S.; Zhang, K.; Panda, G.; Godinho, M.; Martins dos Santos, V.A.; Wang, J. Exploring the metabolic network of the epidemic pathogen *Burkholderia cenocepacia* j2315 via genome-scale reconstruction. *BMC Syst Biol.* **2011**, *5*, 83.

98. Lee, D.S.; Burd, H.; Liu, J.; Almaas, E.; Wiest, O.; Barabási, A.L.; Oltvai, Z.N.; Kapatral, V. Comparative genome-scale metabolic reconstruction and flux balance analysis of multiple *Staphylococcus aureus* genomes identify novel antimicrobial drug targets. *J Bacteriol.* **2009**, *191*, 4015-4024.

99. Rahman, S.A.; Schomburg, D. Observing local and global properties of metabolic pathways: 'Load points' and 'choke points' in the metabolic networks. *Bioinformatics* **2006**, *22*, 1767-1774.

100. Baths, V.; Roy, U.; Singh, T. Disruption of cell wall fatty acid biosynthesis in *Mycobacterium tuberculosis* using a graph theoretic approach. *Theor Biol Med Model* **2011**, *8*, 5.

101. Chaudhury, S.; Abdulhameed, M.D.; Singh, N.; Tawa, G.J.; D'haeseleer, P.M.; Zemla, A.T.; Navid, A.; Zhou, C.E.; Franklin, M.C.; Cheung, J., *et al.* Rapid countermeasure discovery against *Francisella tularensis* based on a metabolic network reconstruction. *PLoS One* **2013**, *8*, e63369.

102. Heinemann, M.; Kümmel, A.; Ruinatscha, R.; Panke, S. In silico genome-scale reconstruction and validation of the *Staphylococcus aureus* metabolic network. *Biotechnol Bioeng* **2005**, *92*, 850-864.

103. Herrgård, M.J.; Fong, S.S.; Palsson, B.Ø. Identification of genome-scale metabolic network models using experimentally measured flux profiles. *PLoS Comput Biol* **2006**, *2*, e72.

104. Kim, H.U.; Kim, S.Y.; Jeong, H.; Kim, T.Y.; Kim, J.J.; Choy, H.E.; Yi, K.Y.; Rhee, J.H.; Lee, S.Y. Integrative genome-scale metabolic analysis of *Vibrio vulnificus* for drug targeting and discovery. *Mol Syst Biol* **2011**, *7*, 460.

105. Raghunathan, A.; Shin, S.; Daefler, S. Systems approach to investigating host-pathogen interactions in infections with the biothreat agent Francisella. Constraints-based model of *Francisella tularensis*. *BMC Syst Biol* **2010**, *4*, 118.

106. Chavali, A.K.; D'Auria, K.M.; Hewlett, E.L.; Pearson, R.D.; Papin, J.A. A metabolic network approach for the identification and prioritization of antimicrobial drug targets. *Trends Microbiol.* **2012**, *20*, 113-123.

107. Fatumo, S.; Plaimas, K.; Mallm, J.P.; Schramm, G.; Adebiyi, E.; Oswald, M.; Eils, R.; König, R. Estimating novel potential drug targets of *Plasmodium falciparum* by analysing the metabolic network of knock-out strains *in silico*. *Infect Genet Evol* **2009**, *9*, 351-358.

108. Guimerà, R.; Sales-Pardo, M.; Amaral, L.A. A network-based method for target selection in metabolic networks. *Bioinformatics* **2007**, *23*, 1616-1622.

109. Chavali, A.K.; Whittemore, J.D.; Eddy, J.A.; Williams, K.T.; Papin, J.A. Systems analysis of metabolism in the pathogenic trypanosomatid *Leishmania major*. *Mol Syst Biol* **2008**, *4*, 177.

110. Perumal, D.; Lim, C.S.; Sakharkar, M.K. A comparative study of metabolic network topology between a pathogenic and a non-pathogenic bacterium for potential drug target identification. *Summit on Translat Bioinforma.* **2009**, *2009*, 100-104.

111. Taylor, C.M.; Wang, Q.; Rosa, B.A.; Huang, S.C.; Powell, K.; Schedl, T.; Pearce, E.J.; Abubucker, S.; Mitreva, M. Discovery of anthelmintic drug targets and drugs using chokepoints in nematode metabolic pathways. *PLoS Pathog* **2013**, *9*, e1003505.

885 112. Ioerger, T.R.; O'Malley, T.; Liao, R.; Guinn, K.M.; Hickey, M.J.; Mohaideen, N.; Murphy, K.C.;
886 Boshoff, H.I.; Mizrahi, V.; Rubin, E.J., *et al*. Identification of new drug targets and resistance
887 mechanisms in *Mycobacterium tuberculosis*. *PLoS One* **2013**, *8*, e75245.
888 113. Orelle, C.; Szal, T.; Klepacki, D.; Shaw, K.J.; Vázquez-Laslop, N.; Mankin, A.S. Identifying the
889 targets of aminoacyl-trna synthetase inhibitors by primer extension inhibition. *Nucleic Acids*
890 *Res* **2013**, *41*, e144.
891 114. Novoa, E.M.; Camacho, N.; Tor, A.; Wilkinson, B.; Moss, S.; Marín-García, P.; Azcárate, I.G.;
892 Bautista, J.M.; Mirando, A.C.; Francklyn, C.S., *et al*. Analogs of natural aminoacyl-trna
893 synthetase inhibitors clear malaria in vivo. *Proc Natl Acad Sci U S A*. **2014**, *111*, E5508-5517.
894 115. Schimmel, P.; Tao, J.; Hill, J. Aminoacyl trna synthetases as targets for new anti-infectives.
895 *FASEB J* **1998**, *12*, 1599-1609.
896 116. Kim, S.; Lee, S.W.; Choi, E.C.; Choi, S.Y. Aminoacyl-trna synthetases and their inhibitors as a
897 novel family of antibiotics. *Appl Microbiol Biotechnol*. **2003**, *61*, 278-288.
898 117. Hurdle, J.G.; O'Neill, A.J.; Chopra, I. Prospects for aminoacyl-trna synthetase inhibitors as
899 new antimicrobial agents. *Antimicrob Agents Chemother*. **2005**, *49*, 4821-4833.
900 118. Thomas, C.M.; Hothersall, J.; Willis, C.L.; Simpson, T.J. Resistance to and synthesis of the
901 antibiotic mupirocin. *Nat Rev Microbiol* **2010**, *8*, 281-289.
902 119. Koh, C.Y.; Siddaramaiah, L.K.; Ranade, R.M.; Nguyen, J.; Jian, T.; Zhang, Z.; Gillespie, J.R.;
903 Buckner, F.S.; Verlinde, C.L.; Fan, E., *et al*. A binding hotspot in *Trypanosoma cruzi* histidyl-
904 trna synthetase revealed by fragment-based crystallographic cocktail screens. *Acta Crystallogr*
905 *D Biol Crystallogr* **2015**, *71*, 1684-1698.
906 120. Biela, I.; Tidten-Luksch, N.; Immekus, F.; Glinca, S.; Nguyen, T.X.; Gerber, H.D.; Heine, A.;
907 Klebe, G.; Reuter, K. Investigation of specificity determinants in bacterial trna-guanine
908 transglycosylase reveals queuine, the substrate of its eucaryotic counterpart, as inhibitor.
909 *PLoS One* **2013**, *8*, e64240.
910 121. Grädler, U.; Gerber, H.D.; Goodenough-Lashua, D.M.; Garcia, G.A.; Ficner, R.; Reuter, K.;
911 Stubbs, M.T.; Klebe, G. A new target for shigellosis: Rational design and crystallographic
912 studies of inhibitors of trna-guanine transglycosylase. *J Mol Biol* **2001**, *306*, 455-467.
913 122. Pohlhaus, J.R.; Long, D.T.; O'Reilly, E.; Kreuzer, K.N. The epsilon subunit of DNA
914 polymerase iii is involved in the nalidixic acid-induced sos response in E*scherichia coli*. *J*
915 *Bacteriol* **2008**, *190*, 5239-5247.
916 123. Cirz, R.T.; Chin, J.K.; Andes, D.R.; de Crécy-Lagard, V.; Craig, W.A.; Romesberg, F.E.
917 Inhibition of mutation and combating the evolution of antibiotic resistance. *PLoS Biology*
918 **2005**, *3*, e176.
919 124. Nautiyal, A.; Patil, K.N.; Muniyappa, K. Suramin is a potent and selective inhibitor of
920 *Mycobacterium tuberculosis* reca protein and the sos response: Reca as a potential target for
921 antibacterial drug discovery. *J Antimicrob Chemother* **2014**, *69*, 1834-1843.
922 125. Culyba, M.J.; Mo, C.Y.; Kohli, R.M. Targets for combating the evolution of acquired antibiotic
923 resistance. *Biochemistry* **2015**, *54*, 3573-3582.
924 126. Tye, B.-K.; Lehman, I.R. Excision repair of uracil incorporated in DNA as a result of a defect
925 in dutpase. *J. Mol. Biol*. **1977**, *117*, 293–306.
926 127. Nguyen, C.; Kasinathan, G.; Leal-Cortijo, I.; Musso-Buendia, A.; Kaiser, M.; Brun, R.; Ruiz-
927 Pérez, L.M.; Johansson, N.G.; González-Pacanowska, D.; Gilbert, I.H. Deoxyuridine

928 triphosphate nucleotidohydrolase as a potential antiparasitic drug target. *J Med Chem* **2005**,
929 *48*, 5942-5954.
930 128. Hampton, S.E.; Baragaña, B.; Schipani, A.; Bosch-Navarrete, C.; Musso-Buendía, J.A.; Recio,
931 E.; Kaiser, M.; Whittingham, J.L.; Roberts, S.M.; Shevtsov, M., *et al.* Design, synthesis, and
932 evaluation of 5'-diphenyl nucleoside analogues as inhibitors of the *Plasmodium falciparum*
933 dutpase. *ChemMedChem* **2011**, *6*, 1816-1831.
934 129. Kepple, K.V.; Boldt, J.L.; Segall, A.M. Holliday junction-binding peptides inhibit distinct
935 junction-processing enzymes. *Proc Natl Acad Sci U S A* **2005**, *102*, 6867-6872.
936 130. Sechman, E.V.; Kline, K.A.; Seifert, S. Loss of both holliday junction processing pathways is
937 synthetically lethal in the presence of gonococcal pilin antigenic variation. *Mol Microbiol* **2006**,
938 *61*, 185-193.
939 131. Suksangpleng, T.; Leartsakulpanich, U.; Moonsom, S.; Siribal, S.; Boonyuen, U.; Wright, G.E.;
940 Chavalitshewinkoon-Petmitr, P. Molecular characterization of *Plasmodium falciparum* uracil-
941 DNA glycosylase and its potential as a new anti-malarial drug target. *Malar J* **2014**, *13*, 149.
942 132. Venkatesh, J.; Kumar, P.; Krishna, P.S.; Manjunath, R.; Varshney, U. Importance of uracil
943 DNA glycosylase in *Pseudomonas aeruginosa* and *Mycobacterium smegmatis*, g+c-rich bacteria,
944 in mutation prevention, tolerance to acidified nitrite, and endurance in mouse macrophages.
945 . *J Biol Chem.* **2003**, *278*, 24350-24358.
946 133. Landini, P.; Corti, E.; Goldstein, B.P.; Denaro, M. Mechanism of action of purpuromycin.
947 *Biochem J* **1992**, *284*, 47-52.
948 134. Nishio, A.; Uyeki, E.M. Cellular uptake and inhibition of DNA synthesis by
949 dihydroxyanthraquinone and two analogues. *Cancer Res* **1983**, *43*, 1951-1956.
950 135. Kelly, T.M.; Stachula, S.A.; Raetz, C.R.; Anderson, M.S. The firA gene of *Escherichia coli*
951 encodes udp-3-o-(r-3-hydroxymyristoyl)-glucosamine n-acyltransferase. The third step of
952 endotoxin biosynthesis. *J Biol Chem.* **1993**, *268*, 19866-19874.
953 136. Raetz, C.R.; Whitfield, C. Lipopolysaccharide endotoxins. *Annu Rev Biochem* **2002**, *71*, 635-
954 700.
955 137. Emiola, A.; George, J.; Andrews, S.S. A complete pathway model for lipid a biosynthesis in
956 *Escherichia coli*. *PLoS One* **2015**, *10*, e0121216.
957 138. Farha, M.A.; Czarny, T.L.; Myers, C.L.; Worrall, L.J.; French, S.; Conrady, D.G.; Wang, Y.;
958 Oldfield, E.; Strynadka, N.C.; Brown, E.D. Antagonism screen for inhibitors of bacterial cell
959 wall biogenesis uncovers an inhibitor of undecaprenyl diphosphate synthase. *Proc Natl Acad*
960 *Sci U S A* **2015**, *112*, 11048-11053.
961 139. Dodbele, S.; Martinez, C.D.; Troutman, J.M. Species differences in alternative substrate
962 utilization by the antibacterial target undecaprenyl pyrophosphate synthase. *Biochemistry*
963 **2014**, *53*, 5042-5050.
964 140. Kuo, C.J.; Guo, R.T.; Lu, I.L.; Liu, H.G.; Wu, S.Y.; Ko, T.P.; Wang, A.H.; Liang, P.H. Structure-
965 based inhibitors exhibit differential activities against *Helicobacter pylori* and *Escherichia coli*
966 undecaprenyl pyrophosphate synthases. *J Biomed Biotechnol* **2008**, *2008*, 841312.
967 141. Zhu, W.; Zhang, Y.; Sinko, W.; Hensler, M.E.; Olson, J.; Molohon, K.J.; Lindert, S.; Cao, R.; Li,
968 K.; Wang, K., *et al.* Antibacterial drug leads targeting isoprenoid biosynthesis. *Proc Natl Acad*
969 *Sci U S A* **2013**, *110*, 123-128.

142. Sinko, W.; Wang, Y.; Zhu, W.; Zhang, Y.; Feixas, F.; Cox, C.L.; Mitchell, D.A.; Oldfield, E.; McCammon, J. Undecaprenyl diphosphate synthase inhibitors: Antibacterial drug leads. *J Med Chem* **2014**, *57*, 5693-5701.

143. Walker, S.; Chen, L.; Hu, Y.; Rew, Y.; Shin, D.; Boger, D.L. Chemistry and biology of ramoplanin: A lipoglycodepsipeptide with potent antibiotic activity. *Chem Rev* **2005**, *105*, 449-476.

144. Helm, J.S.; Hu, Y.; Chen, L.; Gross, B.; Walker, S. Identification of active-site inhibitors of murg using a generalizable, high-throughput glycosyltransferase screen. *J Am Chem Soc* **2003**, *125*, 11168-11169.

145. Mann, P.A.; Müller, A.; Xiao, L.; Pereira, P.M.; Yang, C.; Ho Lee, S.; Wang, H.; Trzeciak, J.; Schneeweis, J.; Dos Santos, M.M., *et al.* Murgocil is a highly bioactive staphylococcal-specific inhibitor of the peptidoglycan glycosyltransferase enzyme murg. *ACS Chem Biol* **2013**, *8*, 2442-2451.

146. Olesen, S.H.; Ingles, D.J.; Yang, Y.; Schönbrunn, E. Differential antibacterial properties of the mura inhibitors terreic acid and fosfomycin. *J Basic Microbiol* **2014**, *54*, 322-326.

147. Bensen, D.C.; Rodriguez, S.; Nix, J.; Cunningham, M.L.; Tari, L.W. Structure of mura (udp-n-acetylglucosamine enolpyruvyl transferase) from *Vibrio fischeri* in complex with substrate udp-n-acetylglucosamine and the drug fosfomycin. *Acta Crystallogr Sect F Struct Biol Cryst Commun* **2012**, *68*, 382-385.

148. Gautam, A.; Rishi, P.; Tewari, R. Udp-n-acetylglucosamine enolpyruvyl transferase as a potential target for antibacterial chemotherapy: Recent developments. *Appl Microbiol Biotechnol.* **2011**, *92*, 211-212.

149. Han, H.; Yang, Y.; Olesen, S.H.; Becker, A.; Betzi, S.; Schönbrunn, E. The fungal product terreic acid is a covalent inhibitor of the bacterial cell wall biosynthetic enzyme udp-n-acetylglucosamine 1-carboxyvinyltransferase (mura) *Biochemistry* **2010**, *49*, 4276-4282.

150. Bachelier, A.; Mayer, R.; Klein, C.D. Sesquiterpene lactones are potent and irreversible inhibitors of the antibacterial target enzyme mura. *Bioorg Med Chem Lett* **2006**, *16*, 5605-5609.

151. Eschenburg, S.; Priestman, M.A.; Abdul-Latif, F.A.; Delachaume, C.; Fassy, F.; Schönbrunn, E. A novel inhibitor that suspends the induced fit mechanism of udp-n-acetylglucosamine enolpyruvyl transferase (mura). *J Biol Chem.* **2005**, *280*, 14070-14075.

152. Smithen, D.A.; Forget, S.M.; McCormick, N.E.; Syvitski, R.T.; Jakeman, D.L. Polyphosphate-containing bisubstrate analogues as inhibitors of a bacterial cell wall thymidylyltransferase. *Org Biomol Chem* **2015**, *13*, 3347-3350.

153. Blankenfeldt, W.; Asuncion, M.; Lam, J.S.; Naismith, J.H. The structural basis of the catalytic mechanism and regulation of glucose-1-phosphate thymidylyltransferase (rmla). *EMBO J* **2000**, *19*, 6652-6663.

154. Lakhal-Naouar, I.; Jardim A, S., R.; Luo S, K., Y.; Nakhasi, H.L.; Duncan, R.C. *Leishmania donovani* argininosuccinate synthase is an active enzyme associated with parasite pathogenesis. *PLoS Negl Trop Dis.* **2012**, *6*, e1849.

155. Piet, J.R.; Geldhoff, M.; van Schaik, B.D.; Brouwer, M.C.; Valls Seron, M.; Jakobs, M.E.; Schipper, K.; Pannekoek, Y.; Zwinderman, A.H.; van der Poll, T., *et al. Streptococcus pneumoniae* arginine synthesis genes promote growth and virulence in pneumococcal meningitis. *J Infect Dis.* **2014**, *209*, 1781-1791.

156. Somvanshi, V.S.; Viswanathan, P.; Jacobs, J.L.; Mulks, M.H.; Sundin, G.W.; Ciche, T.A. The type 2 secretion pseudopilin, gspj, is required for multihost pathogenicity of *Burkholderia cenocepacia* au1054. *Infect Immun.* **2010**, *78*, 4110-4121.

157. Yang, H.L.; Kessler, D.P. Genetic analysis of the leucine region in *Escherichia coli* b-r: Gene-enzyme assignments. *J Bacteriol* **1974**, *117*, 63-72.

158. Singh, R.K.; Kefala, G.; Janowski, R.; Mueller-Dieckmann, C.; von Kries, J.P.; Weiss, M.S. The high-resolution structure of leub (rv2995c) from *Mycobacterium tuberculosis*. *J Mol Biol.* **2005**, *346*, 1-11.

159. Pettit, F.H.; Reed, L.J. Alpha-keto acid dehydrogenase complexes. 8. Comparison of dihydrolipoyl dehydrogenases from pyruvate and alpha-ketoglutarate dehydrogenase complexes of *Escherichia coli*. *Proc Natl Acad Sci U S A.* **1967**, *58*, 1126-1130.

160. Bryk, R.; Arango, N.; Maksymiuk, C.; Balakrishnan, A.; Wu, Y.T.; Wong, C.H.; Masquelin, T.; Hipskind, P.; Lima, C.D.; Nathan, C. Lipoamide channel-binding sulfonamides selectively inhibit mycobacterial lipoamide dehydrogenase. *Biochemistry* **2013**, *52*, 9375-9384.

161. Krauth-Siegel, R.L.; Schöneck, R. Flavoprotein structure and mechanism. 5. Trypanothione reductase and lipoamide dehydrogenase as targets for a structure-based drug design. *FASEB J* **1995**, *9*, 1138-1146.

162. Boitz, J.M.; Strasser, R.; Yates, P.A.; Jardim, A.; Ullman, B. Adenylosuccinate synthetase and adenylosuccinate lyase deficiencies trigger growth and infectivity deficits in *Leishmania donovani*. *J Biol Chem.* **2013**, *288*, 8977-8990.

163. Howard, N.I.; Dias, M.V.; Peyrot, F.; Chen, L.; Schmidt, M.F.; Blundell, T.L.; Abell, C. Design and structural analysis of aromatic inhibitors of type ii dehydroquinase from *Mycobacterium tuberculosis*. *ChemMedChem* **2015**, *10*, 116-133.

164. Cheung, V.W.; Xue, B.; Hernandez-Valladares, M.; Go, M.K.; Tung, A.; Aguda, A.H.; Robinson, R.C.; Yew, W.S. Identification of polyketide inhibitors targeting 3-dehydroquinate dehydratase in the shikimate pathway of *Enterococcus faecalis*. *PLoS One* **2014**, *9*, e103598.

165. Ballester, P.J.; Mangold, M.; Howard, N.I.; Robinson, R.L.; Abell, C.; Blumberger, J.; Mitchell, J.B. Hierarchical virtual screening for the discovery of new molecular scaffolds in antibacterial hit identification. *J R Soc Interface* **2012**, *9*, 3196-3207.

166. Kumar, A.; Siddiqi, M.I.; Miertus, S. New molecular scaffolds for the design of *Mycobacterium tuberculosis* type ii dehydroquinase inhibitors identified using ligand and receptor based virtual screening. *J Mol Model* **2010**, *16*, 693-712.

167. Prazeres, V.F.; Sánchez-Sixto, C.; Castedo, L.; Lamb, H.; Hawkins, A., R.; Riboldi-Tunnicliffe, A.; Coggins, J.R.; Lapthorn, A.J.; González-Bello, C. Nanomolar competitive inhibitors of *Mycobacterium tuberculosis* and *Streptomyces coelicolor* type ii dehydroquinase. *ChemMedChem* **2007**, *2*, 194-207.

168. Siggaard-Andersen, M.; Wissenbach, M.; Chuck, J.A.; Svendsen, I.; Olsen, J.G.; von Wettstein-Knowles, P. The fabj-encoded beta-ketoacyl-[acyl carrier protein] synthase iv from *Escherichia coli* is sensitive to cerulenin and specific for short-chain substrates. *Proc Natl Acad Sci U S A.* **1994**, *91*, 11027-11031.

169. Magnuson, K.; Carey, M.R.; Cronan, J.E.J. The putative fabJ gene of *escherichia coli* fatty acid synthesis is the fabF gene. *J Bacteriol* **1995**, *177*, 3593-3595.

170. Tong, L. Structure and function of biotin-dependent carboxylases. *Cell Mol Life Sci* **2013**, *70*, 863-891.

171. Silvers, M.A.; Robertson, G.T.; Taylor, C.M.; Waldrop, G.L. Design, synthesis, and antibacterial properties of dual-ligand inhibitors of acetyl-coa carboxylase. *J Med Chem* **2014**, *57*, 8947-8959.

172. Reddy, M.C.; Breda, A.; Bruning, J.B.; Sherekar, M.; Valluru, S.; Thurman, C.; Ehrenfeld, H.; Sacchettini, J.C. Structure, activity, and inhibition of the carboxyltransferase β-subunit of acetyl coenzyme a carboxylase (accd6) from *Mycobacterium tuberculosis*. *Antimicrob Agents Chemother* **2014**, *58*, 6122-6132.

173. Levert, K.L.; Waldrop, G.L. A bisubstrate analog inhibitor of the carboxyltransferase component of acetyl-coa carboxylase. *Biochem Biophys Res Commun* **2002**, *291*, 1213-1217.

174. Freiberg, C.; Brunner, N.A.; Schiffer, G.; Lampe, T.; Pohlmann, J.; Brands, M.; Raabe, M.; Häbich, D.; Ziegelbauer, K. Identification and characterization of the first class of potent bacterial acetyl-coA carboxylase inhibitors with antibacterial activity. *J Biol Chem.* **2004**, *279*, 26066-26073.

175. Tong, L. Acetyl-coenzyme a carboxylase: Crucial metabolic enzyme and attractive target for drug discovery. *Cell Mol Life Sci* **2005**, *62*, 1784-1803.

176. Zhang, R.; Ou, H.Y.; Zhang, C.T. Deg: A database of essential genes. *Nucleic Acids Res* **2004**, *32(Database issue)*, D271-272.

177. Moule, M.G.; Hemsley, C.M.; Seet, Q.; Guerra-Assunção, J.A.; Lim, J.; Sarkar-Tyson, M.; Clark, T.G.; Tan, P.B.; Titball, R.W.; Cuccui, J., *et al.* Genome-wide saturation mutagenesis of *Burkholderia pseudomallei* k96243 predicts essential genes and novel targets for antimicrobial development. *MBio* **2014**, *5*, e00926-00913.

178. Somvanshi, V.S.; Viswanathan, P.; Jacobs, J.L.; Mulks, M.H.; Sundin, G.W.; Ciche, T.A. The type 2 secretion pseudopilin, gspj, is required for multihost pathogenicity of *Burkholderia cenocepacia* au1054. *Infect Immun* **2010**, *78*, 4110-4121.

179. van Waasbergen, L.G.; Kidambi, S.P.; Miller, R.V. Construction of a reca mutant of *Burkholderia* (formerly pseudomonas), *cepacia*. *Appl Microbiol Biotechnol* **1998**, *49*, 59-65.

180. Appleberg, R. Macrophage nutriprive antimicrobial mechanisms. *J Leukocyte Biol* **2006**, *70*, 1117-1128.

181. McKinney, J.D.; Bentrup, K.H.; Mun˜ oz-Elias, E.J.; Miczak, A.; Chen, B.; Chan, W.T.; Swenson, D.; Sacchettini, J.C.; Jacobs Jr., W.R.; Russell, D.G. Persistence of *Mycobacterium tuberculosis* in macrophages and mice requires the glyoxylate shunt enzyme isocitrate lyase. *Nature* **2000**, *406*, 735–738.

182. Fang, F.C.; Libby, S.J.; Castor, M.E.; Fung, A.M. Isocitrate lyase (aceA) is required for salmonella persistence but not for acute lethal infection in mice. *Infect. Immun.* **2005**, *73*, 2547–2549.

183. Liu, N.; Cummings, J.E.; England, K.; Slayden, R.A.; Tonge, P.J. Mechanism and inhibition of the fabi enoyl-acp reductase from *Burkholderia pseudomallei*. *J Antimicrob Chemother* **2011**, *66*, 564-573.

184. Bokman, A.H.; Levine, H.B.; Lusby, M. Glucose catabolism in *Malleomyces pseudomallei*. *J Bacteriol* **1957**, *73*, 649-654.

185. Kouassi, Y.; Shelef, L.A. Metabolic activities of *Listeria monocytogenes* in the presence of sodium propionate, acetate, lactate and citrate. *J Appl Bacteriol* **1996**, *81*, 147-153.

186. Premaratne, R.J.; Lin, W.J.; Johnson, E.A. Development of an improved chemically defined minimal medium for *Listeria monocytogenes*. *Appl Environ Microbiol.* **1991**, *57*, 3046-3048.

187. Joseph, B.; Przybilla, K.; Stühler, C.; Schauer, K.; Slaghuis, J.; Fuchs, T.M.; Goebel, W. Identification of *Listeria monocytogenes* genes contributing to intracellular replication by expression profiling and mutant screening. *J Bacteriol.* **2006**, *188*, 556-568.

188. Bordbar, A.; Lewis, N.E.; Schellenberger, J.; Palsson, B.Ø.; Jamshidi, N. Insight into human alveolar macrophage and *M. tuberculosis* interactions via metabolic reconstructions. *Mol Syst Biol* **2010**, *6*, 422.

189. Chatterjee, S.S.; Hossain, H.; Otten, S.; Kuenne, C.; Kuchmina, K.; Machata, S.; Domann, E.; Chakraborty, T.; Hain, T. Intracellular gene expression profile of *Listeria monocytogenes*. *Infect Immun* **2006**, *74*, 1323-1338.

190. Eisenreich, W.; Heesemann, J.; Rudel, T.; Goebel, W. Metabolic host responses to infection by intracellular bacterial pathogens. *Front Cell Infect Microbiol* **2013**, *3*, 24.

191. Caspi, R.; Altman, T.; Dale, J.M.; Dreher, K.; Fulcher, C.A.; Gilham, F.; Kaipa, P.; Karthikeyan, A.S.; Kothari, A.; Krummenacker, M., *et al.* The metacyc database of metabolic pathways and enzymes and the biocyc collection of pathway/genome databases. *Nucleic Acids Res.* **2010**, *38(Database issue)*, D473-479.

192. Joseph, B.; Przybilla, K.; Stühler, C.; Schauer, K.; Slaghuis, J.; Fuchs, T.M.; Goebel, W. Identification of *Listeria monocytogenes* genes contributing to intracellular replication by expression profiling and mutant screening. *J Bacteriol.* **2006**, 556-568.

193. Tuanyok, A.; Tom, M.; Dunbar, J.; Woods, D.E. Genome-wide expression analysis of *Burkholderia pseudomallei* infection in a hamster model of acute melioidosis. *Infect Immun* **2006**, *74*, 5465-5476.

194. Hamad, M.A.; Austin, C.R.; Stewart, A.L.; Higgins, M.; Vázquez-Torres, A.; Voskuil, M.I. Adaptation and antibiotic tolerance of anaerobic *Burkholderia pseudomallei*. *Antimicrob Agents Chemother* **2011**, *55*, 3313-3323.

195. Alberts, B.; Johnson, A.; Lewis, J.; Raff, M.; Roberts, K.; Walter, P. *Molecular biology of the cell, 4th edition*. Garland Science: New York, 2002.

196. Myint, K.T.; Uehara, T.; Aoshima, K.; Oda, Y. Polar anionic metabolome analysis by nano-lc/ms with a metal chelating agent. *Anal Chem* **2009**, *81*, 7766-7772.

197. Lee, I.J.; Hom, K.; Bai, G.; Shapiro, M. Nmr metabolomic analysis of caco-2 cell differentiation. *J Proteome Res* **2009**, *8*, 4104-4108.